ELSEVIER

Journal of Chromatography A, 805 (1998) 177–215

JOURNAL OF CHROMATOGRAPHY A

Pulsed flame photometric detector – a step forward towards universal heteroatom selective detection

Hongwu Jing, Aviv Amirav*

School of Chemistry, Sackler Faculty of Exact Sciences, Tel Aviv University, Tel Aviv 69978, Israel

Received 16 October 1997; received in revised form 30 December 1997; accepted 30 December 1997

Abstract

Pulsed flame photometric detector (PFPD) is characterized by the added information available from flame chemiluminescence emission time dependence. We have found that many elements possess unique delayed emission, whose time dependence can serve for their identification. Since carbon emission is fast and confined to the pulsed flame propagation time across the observation window, the heteroatom delayed emission can be separated in time from that of carbon, resulting in a substantial enhancement in the detection sensitivity and selectivity. For elements with delayed emissions, the PFPD is found to be superior to the conventional FPD in heteroatom detection sensitivity, selectivity against carbon and inter-heteroatom selectivity. Semi-universal heteroatom selective detection is described and illustrated in this paper with 28 elements including carbon. Among all the elements studied, the following elements show unique time-delayed emissions: S, P, N, As, Se, Sn, Ge, Ga, Sb, Te, Br, Cu and In, which enables their specific detection with respect to hydrocarbons. All the other detectable elements including Mn, Fe, Ru, Rh, Cr, Ni, Eu, V, W, B, Si, Al, Pb, Bi and C, show undelayed emissions, and can be selectively detected by the PFPD with a range of sensitivities, and heteroatom against carbon selectivities. The observed sensitivities and selectivities for all the 28 elements that were studied are tabulated and presented. Detailed experimental conditions and analysis data, including pulsed flame emission spectra, pulsed flame emission time dependence, compound used, as well as the chromatographic behavior for each element is provided so that this paper can serve as a comprehensive guiding tool for the universal detection of these elements with the PFPD. The PFPD analysis of methylcyclopentadienyl manganese tricarbonyl as Mn additive in gasoline is shown. In addition, simultaneous heteroatom selective detection and speciation, using a dual-gate response ratio method, is illustrated with a mixture of compounds containing S, Se, As, P, Ge and N atoms.

Keywords: Pulsed flame photometric detection; Flame photometric detection; Detection, GC; Heteroatom-selective detection; Metals; Organometallic compounds; Nitrogen; Phosphorous; Sulfur; Bromine

1. Introduction

The detection of heteroatoms in heteroorganics and/or organometallics with gas chromatography (GC) has experienced more than three decades of research [1–7]. With the ever increasing impact of heteroatoms on our environment and technological development, this area of research has become even more practically significant. For example, the amount of organotin compounds produced worldwide, as polymer stabilizers, ship antifouling coatings or other biocides, doubled in the ten years between 1976 and 1986 [8,9]. Selenium [10] is a typical essential element of biological importance, whose trace exist-

*Corresponding author.

0021-9673/98/$19.00
PII S0021-9673(97)01306-X

ence in animals and humans provides either nutritional or toxic effects depending on its content. Phosphorus, boron, silicon, germanium, gallium and arsenic [11] are widely used by the semiconductor industry. Organometallic compounds of many elements, such as manganese, vanadium, nickel and aluminum, have been used in industry for decades as additives, lubricants, coatings and plating materials, catalysts, corrosion preventers and biocides [12].

Among all of the element selective detectors for GC, the flame photometric detector (FPD) is well known as a selective detector for certain heteroatoms, especially sulfur and phosphorus [13,14]. More than thirty years ago, Juvet and co-workers [1,3,4] had already explored the use of the FPD for the detection of metal chelates and halides with GC. Their pioneering work demonstrated the capability of FPD detection of chromium, iron, rhodium, titanium, arsenic, zirconium, molybdenum, tungsten, tin, aluminum and carbon compounds, with selective or nonselective modes of operation. The detection of many elements has been systematically investigated by Aue and co-workers [9,15–30], using the GC–FPD combination. These include germanium, tin, ruthenium, sulfur, phosphorus, nickel, chromium, iron, manganese, selenium, osmium, boron, arsenic, cobalt, molybdenum, rhenium, antimony, nitrogen, lead, bismuth and carbon. For the FPD detection of chlorine, bromine and iodine, an indium-sensitized flame [13,31–33], copper-sensitized flame [34,35], or sodium-sensitized flame [36] was used. The use of broad bandwidth filters or no filter [4,15], in addition to interference filters, contributed greatly to the FPD element detectability. As is summarized in the literature [25], satisfactory sensitivities for some of the heteroatoms can be achieved, and elemental specificity was demonstrated [25–27,30] with an additional photomultiplier channel. In spite of the above, the FPD is still mostly used as a sulfur–phosphorus detector.

More recently, the commercial emergence of the atomic emission detector (AED) has overshadowed the application of the FPD as a common heteroatom detector. The AED [37,38] appears to be an attractive multi-element selective detector. However, since a plasma excitation source is incorporated and parallel multi-wavelength optical detection equipment is included, the AED is also one of the most expensive detectors for GC. Due to its universal element detectability (for single elements besides helium) and simultaneous detection capability for several elements (typically four), many publications have appeared which describe AED applications. Nevertheless, several problems exist with the AED, such as limited selectivity against carbon, low sensitivity for some nonmetallic elements, discharge tube erosion, high maintenance cost and operation complexity due to a variety of parameter selections [37,39–41].

A pulsed flame photometric detector (PFPD) has recently been developed and described in detail [42–46]. The PFPD is uniquely characterized by the addition of time dependence information of pulsed flame emission. In the PFPD, the combustion of hydrocarbon molecules is highly exothermic and thus fast and irreversible. The flame emission of related radicals, such as CH, C_2 and OH (also from the hydrogen/air flame), is limited to the time duration that is required by the flame front to pass across the photomultiplier window. Heteroatom species such as S_2, HPO and HNO, also emit in the cooler, yet reactive, post pulsed flame conditions due to their lower bond energies. Consequently, their flame emissions are delayed, and can be electronically gated and separated in time from the hydrocarbon and pulsed flame background emissions. As a result, the PFPD detection sensitivities and selectivities with respect to hydrocarbons for sulfur, phosphorus and nitrogen are markedly increased compared with conventional FPDs working with continuous flames. In contrast to the AED, the PFPD is a small, easy-to-use, low cost heteroatom detector. It can be considered as an economical alternative to the AED for the detection of many elements, where it provides satisfactory sensitivity and selectivity. The PFPD is commercially available from both Varian Chromatography Systems and O.I. Analytical.

Having optimized our laboratory-made PFPD structure design and its performance for the three principal heteroatoms, i.e., sulfur, phosphorus and nitrogen [45], an extensive effort was focused on establishing the PFPD as a universal heteroatom selective detector. The results of this research are described here and summarized in Figures and a

Table which outlines the PFPD detectable elements, and their relevant operational parameters and performance.

2. Experimental

A laboratory-made PFPD was mounted on the GC detector base of a Varian 3600 gas chromatograph and was used for all our chromatographic experiments. This PFPD has been described in detail previously [45]. Due to its structural difference and additional glass cover used, the temperature gradient of our PFPD, from its heated base, was smaller than that of the commercial Varian PFPD. Three Hamamatsu photomultiplier tubes (PMTs), R647, R5070 and R1463, were used. With the exception of an Andover 405FS10-25 interference filter with a 10 nm band width for Mn, all other filters were Schott colored glass filters having a 25 mm diameter and 2 mm thickness. Time-delayed emissions of heteroatoms were recorded with a LeCroy 9400 averaging digital oscilloscope. Alternatively, this could be done using later-developed PFPD software [47]. For flame emission spectra, a previous version PFPD [44] was connected to a Jarrell-Ash quarter-meter monochromator with a 38 cm long (5 mm diameter) quartz light guide. The monochromator (gratings blazed at 500 nm), with two 2 mm slits, was fitted with an R1463 PMT. It should be pointed out that all the spectra obtained were uncorrected for both the grating of the monochromator and the PMT spectral responses. Schott colored glass filters, such as WG335 or WG360, were used for some elements to prevent second-order dispersion from entering their flame emission spectra. In order to introduce a pure heteroatom compound for the recording of flame emission spectra, a stainless steel tee with a glass vial containing the compound, was connected to a short capillary column and placed inside the GC oven. In this way it became a temperature-controlled micro-evaporator, which was then operated at the minimum temperature required. After removing the used vial, the stainless steel tee was cleaned with dilute nitric acid, rinsed with distilled water and organic solvents, and baked on-line in the GC oven until it was found to be free from any residue of the previous element in memory-test runs. In addition, the PFPD quartz combustor was checked to be fully transparent before and after recording the spectrum of each element that could form an internal oxide deposit. A simultaneous channel of pulsed flame ionization detection (PFID) [46] was combined with this PFPD in its upper igniter chamber. It served as a trigger source for the pulsed flame emission measurement through the monochromator.

Three mm I.D. quartz combustors were preferentially used with the PFPDs for elements exhibiting a linear response. Otherwise, 2 mm I.D. combustors were used for elements exhibiting a quadratic response.

A Varian FID for Varian 3600 GC was used for calibration and comparison. A simple switching of the column output between the PFPD and the FID made this evaluation possible under the exact same injection conditions. The calibration of some heteroatoms with the FID was necessary for calculating the real amount of heteroatom compounds that entered the PFPD, which was then used in both sensitivity and selectivity evaluation. As the FID is a standard detector for FID-active carbon content, the comparison between its chromatogram and the PFPD chromatogram demonstrated the PFPD heteroatom selectivity.

The heteroatom compounds were purchased from Aldrich, Strem Chemicals, Merck, Fluka and Alfa, and used as received. Anhydrous solvents were used to prepare stock solutions when necessary. The concentration of each component in a solution was given in either w/v or v/v depending on whether the material was a solid or liquid at room temperature. Therefore, the sensitivities and selectivities reported in this paper are given with no density correction when a liquid compound was used.

Helium was always used as the carrier gas. Unless otherwise indicated, 4 m×0.25 mm I.D., J&W DB-1 columns with 0.25 μm film thickness were used in this study, in order to minimize the dissociation of some thermally labile compounds. In such cases, a high column flow-rate and large split gas flow-rate were adopted as well.

It ought to be noted that throughout this study a small industrial ventilation pump with sufficient pumping ability was mounted above the PFPD gas

outlet to remove harmful exhaust gases and the GC split output was connected to a split vent trap in a hood.

3. General results and discussion

The detection of 28 elements was tested with the PFPD. Based on the time dependence of their flame chemiluminescent emission, these elements can be divided into two categories. The first group includes S, P, N, As, Se, Sn, Ge, Ga, Sb, Te, Br, Cu and In, which show time-delayed emissions that allow their specific detection with respect to hydrocarbons. The second group includes Mn, Fe, Ru, Rh, Cr, Ni, Eu, V, W, B, Si, Al, Pb and Bi, which show undelayed emissions, and can be selectively detected by the PFPD with a range of sensitivities, and heteroatom against carbon selectivities. In addition, carbon can be universally detected with the PFPD, which serves as an FID-like carbon channel.

Fig. 1 shows the PFPD detectable elements in the periodic table including their detection limits and selectivity against carbon. It can be seen from this Figure that most of the main group elements in the vicinity of arsenic, which happened to have the longest delayed emission, are detectable. In total, 13 elements exhibited time-delayed emission and therefore their selectivities against carbon are much better than with conventional FPDs. The time dependency

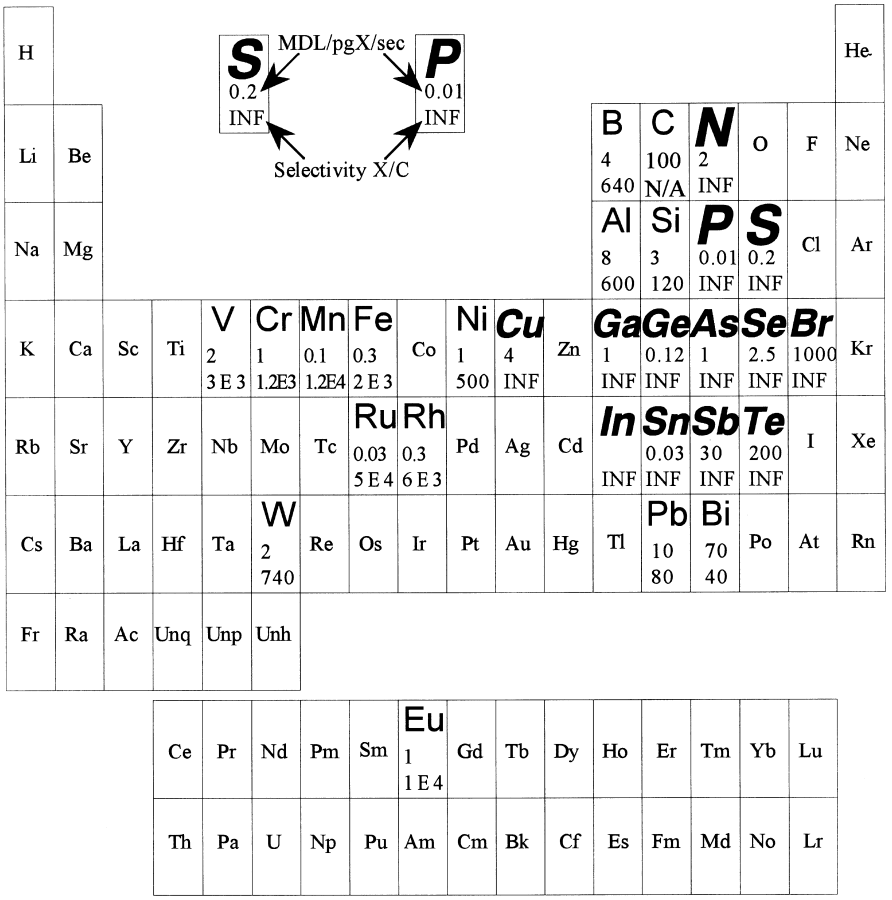

Fig. 1. The PFPD periodic table. The elements which are detectable with the PFPD are written in large font size. Those elements shown in bold face exhibit time-delayed emissions and thus have infinite (INF) selectivities. The minimum detection levels (in pg element per second) and selectivities against carbon are shown under the element. Examples for S and P are shown at the top.

of the delayed emissions for all of these elements seems to be related to the medium bond strength of the emitting species. When strong bonds were formed in the flame chemiluminescent species, such as with C, B and Si, the emission was fast and irreversible and thus only undelayed emission was observed. When the radical bond strength was low, it was unstable and thus its flame emission was weak or absent. We believe that the halogens are representative of this scenario. Since, in the detection of elements with delayed emissions, the combustible gas composition of the PFPD is usually hydrogen-rich, hydrogen-involving reactions of these heteroatoms probably relates to the formation of their flame chemiluminescent species. Within the same group, those elements which are intermediate in position possess intermediate chemical bond strengths in the emission species and thus exhibit longer time-delayed emissions; those located on the upper side possess greater bond strengths and thus exhibit shorter or undelayed emissions; and those located on the lower side possess lower bond strengths, therefore, they might exhibit time-delayed emission but presumably with small population of their flame emission species and thus poor emission intensity. For instance, in group VA, As is the intermediate element that possessed the longest delayed emission. Moving upward from As to N, the emission delay reduces, therefore, N exhibited a very short time-delayed emission. On the other hand, Bi did not exhibit delayed emission since it was assumed to be very weak. In the halogen series, bromine exhibited best time-delayed emission; chlorine exhibited hardly any emission (either delayed or undelayed emission), and iodine exhibited a very weak time-delayed emission. It is worthwhile to note that there is no simple correlation between the time delay and the intensity of the pulsed flame emission. Fortunately, all of the analytically more important elements such as S, P, N, As, Sn, Se and Ge are characterized by delayed pulsed flame emission.

The other 14 elements with undelayed emissions were detected with selectivities between 40 and 50 000. Compared with conventional FPDs, the PFPD demonstrated better sensitivities (up to 100 times) for several heteroatoms with undelayed emissions. This increase in sensitivity may originate from a combination of the higher peak temperature of the pulsed flame, a better PMT for red emission or additional unknown reasons. While V and W showed good PFPD response, they were found to be very poor with the FPD [25]. Additionally, several other elements have been successfully detected with conventional FPD as a GC detector. These elements include Ti, Zr, Mo, Co, Os and Re [3,4,23,29], which were not tested with the PFPD.

Cl, Br and I can be detected through indium sensitized flame chemiluminescence and was successfully employed using the PFPD with delayed emission (infinite selectivity) and good sensitivity (1–10 pg X/s). However, long term instability, and cleaning difficulty for renewed phosphorus detection occurred due to In amalgamation. Indium has a delayed emission and can probably be effectively detected by the PFPD through its indium hydride lines (with a GG495 filter). Hg, Zn, Cl and F did not yield any noticeable flame emission in the PFPD, while I exhibited a very weak emission. Neither H nor O are detectable with the PFPD from a practical standpoint, as they are the source of the flame. In addition, due to the lack of volatile organic compounds of alkali and alkaline earth elements, no effort was made for their detection with the PFPD even though conventional flame photometers are widely used for these elements.

The experimental conditions and detection parameters for the PFPD detection of all the elements studied are summarized in Table 1:

1. Element (X)/compound used: the elements are given together with the compound used in cases where only one compound was used. When more than one compound were used we omit the names (represented by ''many''). acac=Acetylacetonate, Ph=phenyl, thd=tetramethyl heptane-dionate, MMT=methylcyclopentadienyl manganese tricarbonyl.
2. Emission time (denoted as ET): D indicates delayed emission while U indicates undelayed.
3. Gases: this is the combustible gas composition of the PFPD. H, S and A indicate a hydrogen-rich, near stoichiometric, and air-rich H_2/air mixture, respectively. In a near stoichiometric H_2/air mixture, the O_2/H_2 ratio is close to 0.5. In a hydrogen-rich or air-rich H_2/air mixture, the O_2/H_2 ratio is less and greater than 0.5, respectively. However, there is a relatively broad range of gas

Table 1
Element selective detection conditions with the PFPD

Element (X)/ compound used	ET	Gases	Filter	PMT	Combustor I.D. (mm)	Peak shape	*T* (°C)	RL	X/C selectivity	Sensitivity (pg X/s)
Aluminum $Al(acac)_3$	U	S	GG495	R647	3	clean	320	L	600	8
Antimony $Sb(OC_2H_5)_3$	D	H	OG590 GG495	R5070 R647	3	tail (reduced)	200–350 200	L	I	30 60
Arsenic $As(Ph)_3$	D	H	RG695 GG495	R5070 R647	3	tail (reduced)	350 200	L	I	1 3
Bismuth $Bi(Ph)_3$	U	S, A	GG495 OG590	R647 R1463	3	clean	280	L	40	70 100
Boron $B(OC_3H_7)_3$	U	A	GG495	R647	3	clean	200–350	L	640	4
Bromine many	D	H	RG9	R5070	2	clean	200	Q	I	1000
Carbon many	U	H A	BG12	R647	3	clean	200 200–350	L	N.A.	200 100
Chromium $Cr(acac)_3$	U	S, A	GG495	R647	3	clean	300	L	1200	1
Copper $Cu(acac)_3$	D	H S	OG590 GG495	R5070 R647	3	clean	280	L	I	4
Europium $Eu(thd)_3$	U	S, A	OG590	R1463	3	clean	280	L	10^4	1
Gallium $Ga(acac)_3$	D	H	OG550	R647	3	clean	200	L	I	1
Germanium $Ge(C_2H_5)_4$	D	H	OG590	R5070	3	clean	200–350	L	I	0.12
Iron Ferrocene	U	S, A	GG495	R647	3	clean	300	L	2000	0.3
Lead $Pb(Ph)_4$	U	S, A	BG12	R647	3	clean	200–350	L	80	10
Manganese MMT	U	S, A	IF403 BG12	R647	3	tail (<5%)	200	L	$1.2\cdot10^4$ 3000	0.1
Nickel Nickelocene	U	S, A	GG495	R647	3	clean	300	L	500	1
Nitrogen many	D	H	RG9 GG495	R5070 R647	3	clean	250	L	I	2 200
Phosphorus many	D	H	GG495	R647	3	clean	300	L	I	0.01
Rhodium $Rh(acac)_3$	U	S, A	GG495	R647	3	clean	300	L	6000	0.3
Ruthenium Ruthenocene	U	S	OG590 GG495	R5070 R647	3	clean	350	L	$5\cdot10^4$	0.03

Table 1. Continued

Element (X)/ compound used	ET	Gases	Filter	PMT	Combustor I.D. (mm)	Peak shape	*T* (°C)	RL	X/C selectivity	Sensitivity (pg X/s)
Selenium $Se(Ph)_2$	D	H	BG12	R647	2	clean	200	Q	I	2.5
Silicon many	U	A	GG495	R647	3	clean	300	L	120	3
Sulfur many	D	H	BG12	R647	2	clean	200–250	Q	I	0.2
Tellurium $Te_2(Ph)_2$	D U	H S	GG495 BG12	R647	2 3	clean	220	Q L	I 150	200 3
Tin $Sn(C_2H_5)_4$	D	H	BG12 OG590	R647	3	tail (reduced)	350 150	L	I	0.03
Tungsten $W(CO)_6$	U	S	GG495	R647	3	clean	280	L	740	2
Vanadium $V(acac)_3$	U	S, A	OG590 RG9	R1463	3	clean	320	L	3000 8000	2 5

composition in the PFPD for its near optimal operation for the detection of each element. The gas distribution in the PFPD is usually more hydrogen-rich in its combustor and more air-rich in its igniter chamber as previously reported for sulfur, phosphorus and nitrogen detection [44,45]. The PFPD gas composition is fundamental to the pulsed flame chemical reaction, and different flame chemiluminescent species can therefore form in different pulsed flame environments. The PFPD gas composition may affect the pulsed flame temperatures and element analytical performance including the emission spectrum, response linearity, sensitivity, selectivity and GC peak shape. Note that even though the same symbols, H, S and A, are used, they may imply different pulsed flame gas composition depending on the element.

4. Filters: a recommended set of filters includes: (a) BG12 for S and many other elements. (b) GG495 for P and many other elements. (c) RG9 for N and Br. (d) WG345 for multi-element detection. (e) BG39 for P detection without nitrogen with R5070 PMT. (f) OG590 for Ge, Se, Bi, Cu, Eu and Sn to enhance selectivity. (g) RG695 for As optimal detection. (h) OG550 for Ga. (i) GG455 and RG645 for further general optimization. (j) Interference filter for Mn, maximum wavelength centered around 403 nm (or 405 nm) with 10 nm band width. (k) BG1 for simultaneous S plus N detection without P interference or chemical noise. Thus a set of 12 filters can be used for all 28 elements.
5. Photomultipliers (PMTs): R647 or R5070 were routinely used. Our R5070 PMT gain seemed to be slightly unstable displaying some gain beating with the PFPD frequency. Care must be taken to stabilize the high voltage power supply in order to avoid 50 Hz gain fluctuation. Thus, for undelayed red emission detection we used R1463. Nevertheless, R5070 can be used instead of R1463.
6. Combustor I.D.: 3 mm I.D. is preferred for general use. However, 2 mm I.D. is preferred for elements with quadratic behavior (S, Se, Te, Br). However, even with these elements a 3 mm I.D. combustor is preferred when quenching limits the analyzed sample amount (e.g., sulfur in gasoline).
7. GC peak shape: peak tailing was observed with As, Sb and Sn. Either a higher or lower PFPD temperature could be used to reduce peak tailing. When the PFPD base temperature was increased to 350°C or slightly higher, the peak tail could usually be reduced to a tolerable limit. Otherwise, lower PFPD temperatures such as 200°C or even 150°C could be used to reduce the peak tail amplitude to a very low level but with long

recovery time. A few other elements like Mn showed minor residual tailing that was long and with low amplitude.

8. Temperature (T) (°C): our PFPD was thermally insulated by a glass cover and is shorter than Varians commercially available PFPD. Thus, the body temperatures of our PFPD usually corresponded to higher temperatures than the Varian PFPD with same base temperatures. The temperature is only a recommendation for optimal PFPD operation, and can also depend on the compound volatility.
9. Response linearity (RL): L indicates a linear response while Q indicates a quadratic response. For most elements only a narrow range of linearity was explored.
10. Selectivity (X/C). A delayed gate enables infinite selectivity (denoted with ''I'' in the selectivity column in Table 1) against hydrocarbon, but interference from other elements with delayed emissions may appear depending on the filter and gate delay used. For heteroatoms that had a linear response and undelayed emission, the heteroatom (X) against carbon (C) selectivity (X/C) was defined as: $X/C=[P(X)/P(C)][I(C)/I(X)][c(C)/c(X)]$, where $P(X)$ and $P(C)$ were the PFPD peak heights of heteroatom and hydrocarbon compounds, respectively, $I(X)$ and $I(C)$ were the FID peak heights of heteroatom and hydrocarbon compounds, respectively, and $c(C)$ and $c(X)$ were the FID valid carbon and the heteroatom contents in the heteroatom compound, respectively. Therefore, the selectivity (X/C) was actually the PFPD response ratio between heteroatom (weight in grams) and carbon (weight in grams) with an FID calibration for carbon content correction. The FID calibration was required due to several factors, such as dissociation or solvent involved ligand substitution in solution, compound thermal lability and injector or column trapping of heteroatom compounds, that could affect their actual introduction into the detectors.
11. Sensitivity (pg X/s). The sensitivity is represented in minimum detection level (MDL), which was evaluated from an extrapolation based on 2 RMS noise and given in picograms of element per second. The FID calibrated heteroatom concentration was used due to the reasons mentioned above. We used 2 RMS noise as the limiting noise. For two peak-to-peak noise the values should be multiplied by 2.8, for elements with linear response, and 1.7 for the elements with quadratic response. For several elements, the MDL can probably be further improved by careful optimization.

3.1. PFPD selective detection of elements with time-delayed emissions

Elements with delayed emissions can be detected with the PFPD with excellent selectivities, and with a range of sensitivities. The pulsed flame used for obtaining optimal delayed emission with these elements was usually hydrogen-rich as used with sulfur and phosphorus, and thus lower in temperature. The chemiluminescent species are typically diatomic molecules, such as S_2, Se_2 and Te_2, for those elements which exhibit a quadratic response, and hydrogen species for many others, such as HPO, HNO for P, N and hydrides for SnH, GeH.

3.1.1. Phosphorus, sulfur and nitrogen

Phosphorus and sulfur are the two most important elements for the PFPD due to their abundant existence in nature and many existing detection applications. These elements have been studied in detail as described previously [44,45]. These references also describe the PFPD selective detection of nitrogen via its HNO flame chemiluminescence.

Nitrogen selective detection via its HNO flame chemiluminescence, using an R5070 PMT and RG9 filter, is the optimal choice [44,45]. However, nitrogen can also be selectively detected and/or identified with the R647 PMT that is used for sulfur and phosphorus and normally provided by the PFPD manufacturers if a nitrogen mode is not requested.

Fig. 2 shows the PFPD undelayed emission spectrum of nitrogen with a peak at 385 nm due to the CN emission band. We noted that this spectrum is not the same as that reported for a conventional FPD [26]. While the section with wavelength greater than 650 nm was found predominantly from the second-order dispersion of the monochromator, a portion of it might result from the HNO emission species that was attributed to the source of time-delayed emission of nitrogen in the PFPD [44].

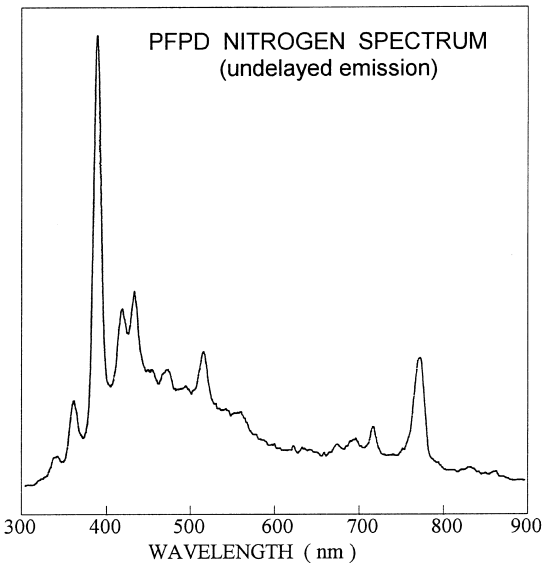

Fig. 2. Undelayed emission spectrum of nitrogen in a pulsed flame. Pyridine was used as the nitrogen source. A slightly air richer gas mixture (in comparison with sulfur) was provided for the PFPD. The section with wavelength greater than 650 nm was found to be predominantly from the second-order dispersion of the monochromator.

As shown in Fig. 3, using the available phosphorus GG495 filter, R647 PMT, quartz combustor and electronic measurement gate, nitrogen was detected with a weak delayed emission (trace B) with an MDL of 200 pg N/s which is two-orders of magnitude higher than with the normal red emission. This delayed emission improves the selectivity of nitrogen over carbon. On the other hand, considering the normal phosphorus detection MDL of the PFPD in this P-mode operation of about 0.01 pg P/s, its P/N inter-heteroatom selectivity is greater than 10^4. This is much greater than the typical P/N selectivity (<10) of the nitrogen–phosphorus detector (NPD) [48]. Nitrogen can also be detected under these conditions with an undelayed short gate (trace C) with an MDL of 20 pg N/s, which is only one-order of magnitude worse than that under optimal conditions. The N/C selectivity observed was 40. The optimal gas composition for this mode required slightly more air than in the normal phosphorus mode.

Although we did not test it, this nitrogen mode should be useful in the detection of inorganic NO_x, NH_3 and H_2N_2 assuming that the emitting species are not CN. This mode can also assist in nitrogen heterocyclic compound identification by direct comparison with the FID traces.

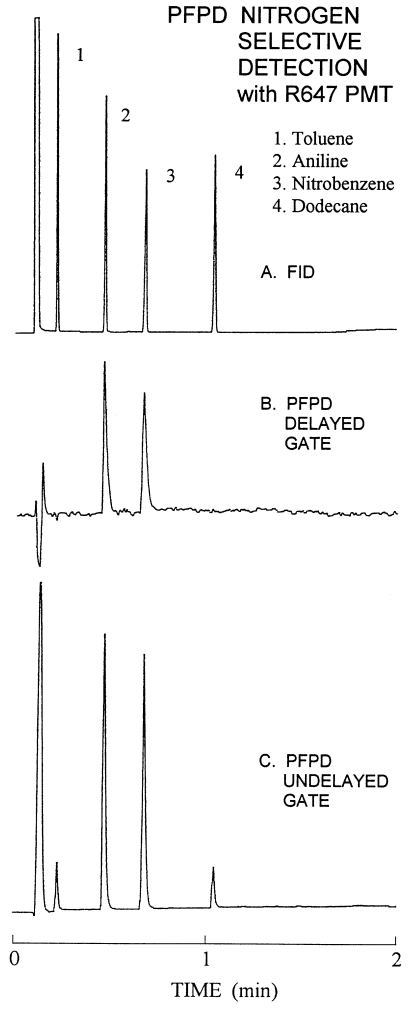

Fig. 3. Nitrogen selective detection with the PFPD under phosphorus optimal detection conditions. 0.5 μl of an ethanol solution of toluene, aniline, nitrobenzene and dodecane with a concentration of $3 \cdot 10^{-3}$ each was injected with a split ratio of 50:1. The column temperature was ramped from 60 to 150°C at 50°C/min. The PFPD base temperature was set to 200°C. A GG495 filter and R647 PMT were used.

3.1.2. Arsenic

Arsenic exhibits several unique features that distinguish it from S, P, C and N and enable selective

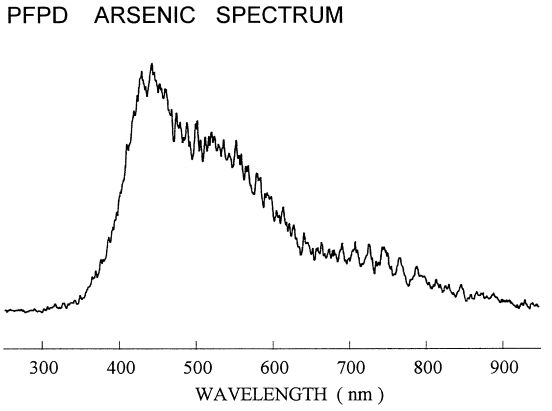

Fig. 4. PFPD time-delayed emission spectrum of arsenic. Triphenylarsine was introduced into the PFPD at 160°C. The PFPD gas composition used was 18 ml/min of air and 7 ml/min of hydrogen. Since only the time-delayed emission was recorded, no filter was used, and the undelayed flame background and hydrocarbon emissions were excluded.

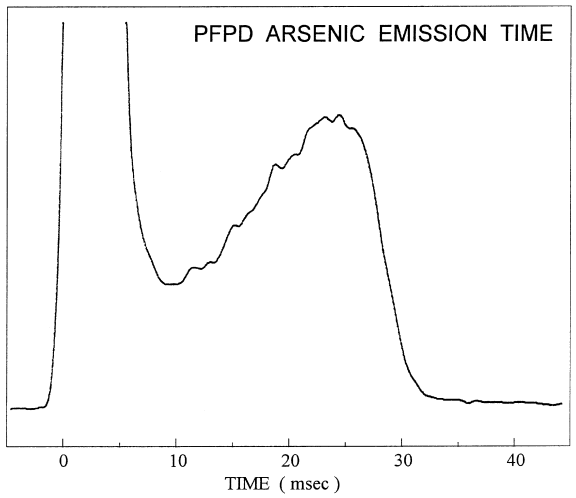

Fig. 5. Time dependence of arsenic emission in a pulsed flame. The profile was recorded with a LeCroy 9400 digital oscilloscope. The PFPD was used with an RG695 filter and R5070 PMT. Note that the emission of arsenic exhibits a very long time delay with a unique emission maximum located at its long time portion. The large emission at the main flame background position (before 6 ms) contains undelayed arsenic emission.

detection which can be optimized for a given application.

As shown in Fig. 4, arsenic emitted a spectrum similar to that of white light, covering the 360–800 nm visible range. The PFPD combustor could easily have been coated if the introduction rate of the triphenylarsine was too high. If this coating had occurred, it would have poisoned the combustor and diminished the time delay of arsenic emission. Thus, a relatively small amount of the arsenic source compound was introduced into the PFPD, resulting in a low signal-to-noise (S/N) ratio in the spectrum. (This coating was slowly self-cleaned). Nevertheless, it can be seen from the spectrum that many filters could have been selected. The choice of a filter is then dependent upon what other elements should be avoided or simultaneously detected. The use of an RG695 filter with R5070 PMT was the best, both in terms of sensitivity and minimal S and P interference. Phosphorus and/or nitrogen interference can be greatly reduced by using a very long delay, but sulfur elimination is more difficult and requires a dual gate approach [45] or an air-rich gas composition.

We note that arsenic is characterized by the longest emission time delay observed, even further delayed than sulfur, with its emission maximum being shifted to very long times. Thus, the 20 ms gate width for sulfur can be employed but preferably with an even larger delay. The emission of arsenic under hydrogen-rich conditions is shown in Fig. 5. Both $As(C_6H_5)_3$ and $AsCl_3$ were used, and provided the same delayed emission.

Hydrogen-rich gas compositions like those for sulfur or phosphorus can be used for optimizing the delayed emission. Under near stoichiometric conditions the emission delay was reduced but this mode improves the selectivity against sulfur or phosphorus. A 3 mm I.D. combustor was preferred and resulted in 1.5-times better sensitivity than a 2 mm I.D. combustor.

Arsenic showed GC peak tailing as demonstrated in Fig. 6. Traces B, C and D shows the selective detection of arsenic with the PFPD under different gate and temperature conditions. The tailing depended on the combustor conditions and annealing history, and might change somewhat in time. It was slightly better with RG695 filter/R5070 PMT than with a BG12 filter. Although a 300°C PFPD base temperature was practically acceptable as with phosphorus, the peak tail was further reduced at higher temperatures. The tail can be further reduced to a

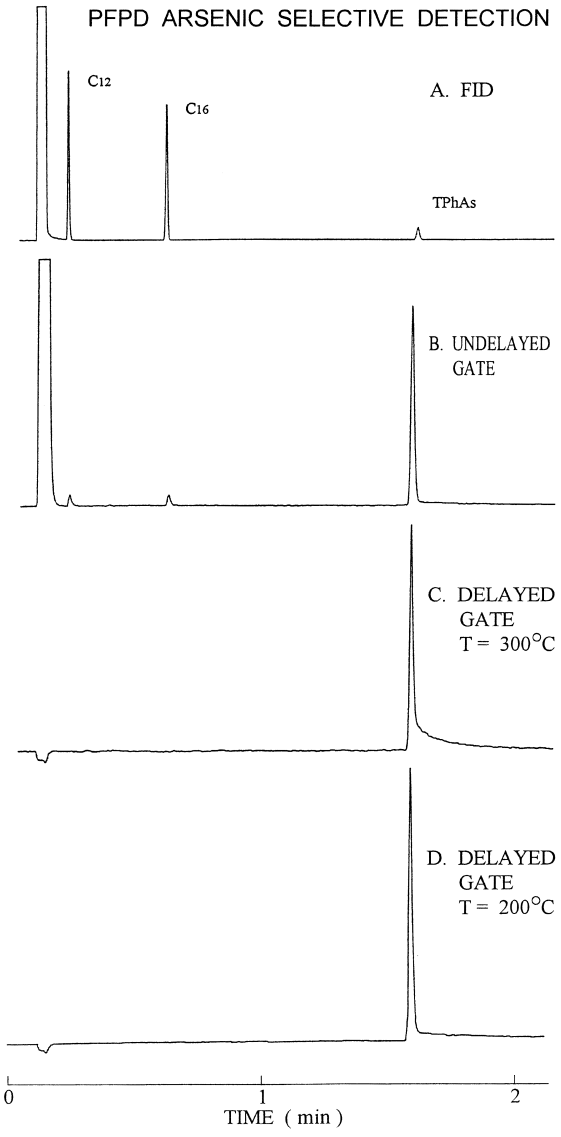

Fig. 6. Arsenic selective detection with the PFPD. 0.5 μl of a solution of $1.3 \cdot 10^{-4}$ triphenylarsine, and $1 \cdot 10^{-3}$ dodecane and hexadecane was injected with a split ratio of 40:1. The column temperature was ramped from 135 to 250°C at 50°C/min. An RG695 filter and R5070 PMT were used in traces C and D while a GG495 filter and R647 PMT were used in trace B. The PFPD base temperature was 300°C for traces B and C, and 200°C for trace D.

small magnitude with a longer decay time at a PFPD temperature of 200°C as shown in trace D. Thus, 200°C is recommended for achieving a chromatogram with a longer but lower magnitude tail. At low PFPD temperatures the emission was separated to a fast tail free component and a tail that became long but with reduced amplitude.

Using an air-rich gas composition and undelayed gate (as in the carbon mode) in conjunction with a GG495 filter, the PFPD provided good sensitivity of around 1 pg As/s, with almost no peak tailing. However, it came with a penalty of reduced As/C selectivity of about 700 as demonstrated in trace B of Fig. 6, similar or slightly better than that obtained with conventional FPDs [15,49]. This mode seemingly solves the sulfur interference problems. It may involve AsC species and thus AsH_3 might not be detected, but this hypothesis was not tested.

We obtained an MDL of 1 pg As/s with 2 RMS noise (3 pg As/s with 2 peak-to-peak noise) using an RG695 filter/R5070 PMT. Using the phosphorus or sulfur mode filters gave a slightly higher MDL of ~3 pg As/s. Fig. 6 was obtained with 1.6 ng $As(C_6H_5)_3$ and 12 ng hydrocarbons.

Heteroatom interference can be minimized with the RG695 filter/R5070 PMT. A very long time delay of up to 20 ms helps to reduce sulfur interference, as well as to eliminate phosphorus and/or nitrogen interference. Quenching limits the injected amount in the case of very complex mixtures such as petrochemical fluids. The sulfur interference is from HSO red emission that is linear with the sulfur concentration and does not disappear even with an air-rich gas composition. A good GC separation is helpful in solving or reducing these problems.

3.1.3. Selenium

Selenium can be detected with the PFPD under practically the same conditions as sulfur with about an order of magnitude higher minimum detection level (two-orders of magnitude lower signal). It is thus appropriate to apply most aspects of sulfur detection conditions to selenium detection.

In Fig. 7 we show the broad spectrum of Se_2 time-delayed emission which covered the 360–550 nm spectral range. A similar band resulting from continuous flames was reported in the literature [16,50].

As shown in Fig. 8, the selenium emission was characterized by a very long delay, similar but slightly shorter than that of sulfur. Thus, the same gate, as that used for sulfur, can be used. Selenium exhibited quadratic response dependence on con-

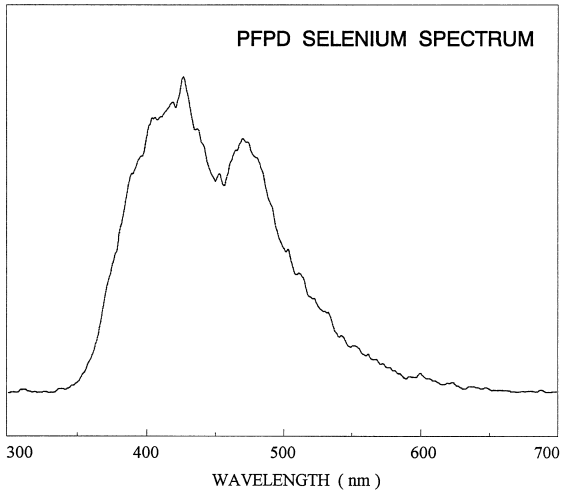

Fig. 7. PFPD time-delayed emission spectrum of selenium. Diphenyl selenide was introduced into the PFPD at 90°C.

centration similar to sulfur as the emitting species is Se_2. It also exhibited a prompt, undelayed emission.

The best sensitivity was achieved with a BG12 filter due to lower noise in that range. The WG345 filter enabled a signal increase by a factor of almost 3 but the noise was increased by a factor of 5, thus the MDL was increased by about 1.3. The GG495 filter provided about the same signal as with the BG12, but the noise was 3.6-times higher and thus the MDL was almost 2-times higher with the advantage of reduced sulfur interference by a factor of about 30. Thus, it is recommended to use the GG495 filter if sulfur response is undesirable.

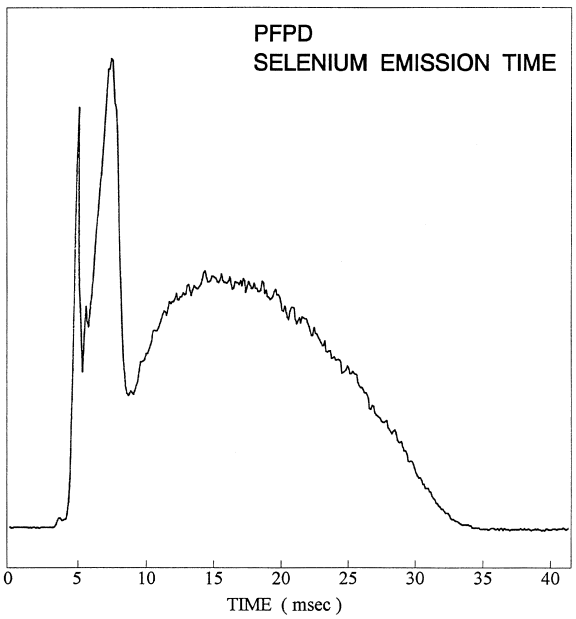

Fig. 8. Time dependence of selenium emission in a pulsed flame. The PFPD was used with an R647 PMT and WG345 filter.

The PFPD gas composition for Se was optimized with hydrogen-rich conditions as that for sulfur. Similarly, a 2 mm combustor was preferred as with sulfur. With a 3 mm I.D. combustor, the S/N ratio was reduced by a factor of about 1.8. We used 200°C PFPD temperature since the S/N ratio was reduced at higher PFPD temperatures as with sulfur.

As shown in Fig. 9 no peak tailing was observed, and Se provided very clean peak shape. We found an MDL of 2.5 pg Se/s, and infinite selectivity, i.e., specific response against hydrocarbons. Note that the selectivity of selenium against sulfur was poor and at a similar concentration the sulfur signal was over 100-times higher than the selenium signal. The delayed emission time was very similar and could not be easily used to distinguish between the emitting species. However, we found that under certain air-rich conditions, selenium, in contrast to sulfur, also had an undelayed emission which was linear to its concentration and enabled an MDL of about 6 pg Se/s. The comparison of ''carbon-like'' prompt emission, and delayed gate normal traces enabled S and Se identification as demonstrated in Fig. 10.

3.1.4. Tin

Tin can be selectively detected with the PFPD with extremely high sensitivity and selectivity without any hydrocarbon interference. Tin did, however, exhibit peak tailing that was reduced to an acceptable level at high detector temperatures. Alternatively, at 150°C the tail was so long that it was barely observed. Nevertheless, it was self-cleaned, before the next run, within about 10 min.

As can be seen from Fig. 11, tin exhibited an emission spectrum with a broad feature at 380–540 nm which has been attributed to its interaction with the combustor quartz surface [18]. In addition, it showed a sharp band at 610 nm and a smaller one at 695 nm that were identified as SnH emissions [9,18].

As shown in Fig. 12, tin produced a unique emission time delay that was longer than that of

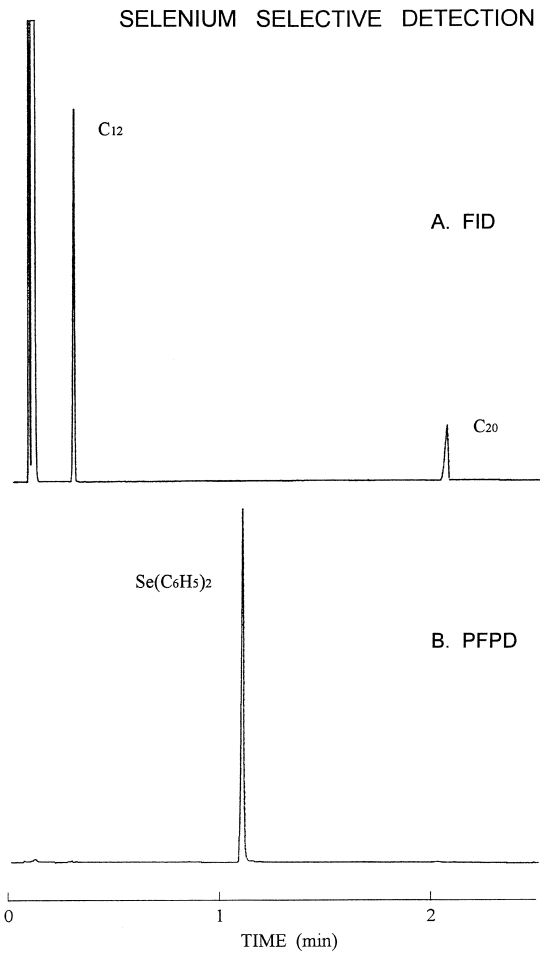

Fig. 9. Selenium selective detection with the PFPD. 0.4 μl of a solution of $4 \cdot 10^{-5}$ diphenyl selenide, 1.5% dodecane and 0.5% eicosane was injected with a split ratio of 40:1. The column temperature was set to 120°C for 0.5 min, and then ramped to 250°C at 50°C/min. A 2 mm I.D. combustor, 20 ms wide delayed gate, BG12 filter and R647 PMT were used with the PFPD. The base temperature of the PFPD was 200°C.

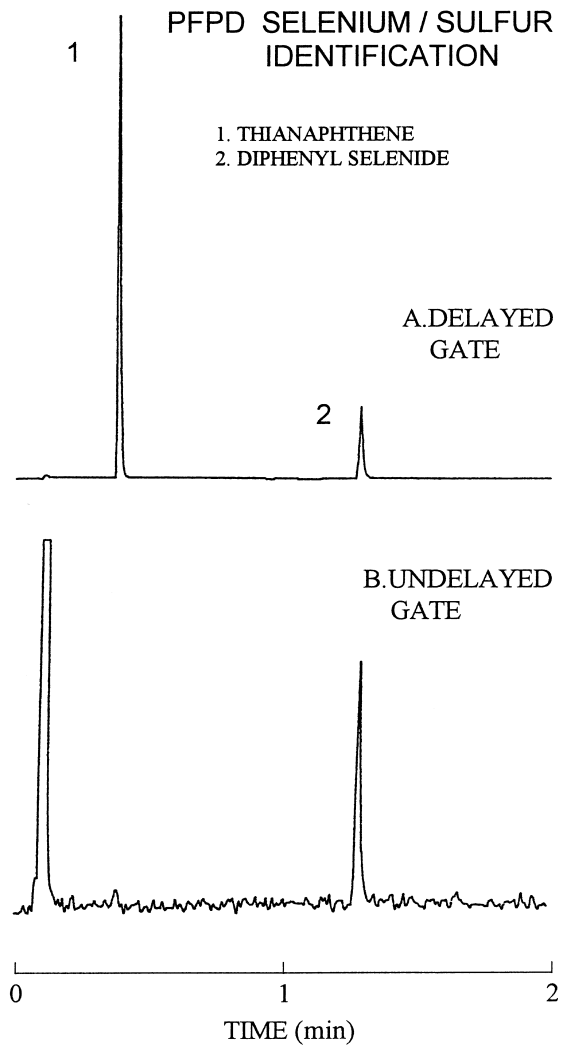

Fig. 10. Selenium and sulfur identification with the PFPD. 0.7 μl of an ethanol solution of $3 \cdot 10^{-6}$ thianaphthene and $2 \cdot 10^{-5}$ diphenyl selenide was injected with a split ratio of 50:1. The column temperature was ramped from 100°C to 180°C at 40°C/min. An undelayed narrow gate was used for trace B. The rest of the conditions were as in Fig. 9.

phosphorus but shorter than that of sulfur. At lower temperatures this emission time delay was increased (trace B). The time-delayed emission of tin was observed at all wavelengths.

The best sensitivity was achieved with a BG12 filter and was higher, by a factor of about four, than with an OG590 filter at the SnH band using an R647 PMT. With an R5070 PMT the reduction factor with the OG590 filter was only two. This latter combination produced a better selectivity against sulfur.

A 3 mm I.D. combustor was preferred but the performance was only slightly better than with a 2 mm I.D. combustor. Tin detection was optimized with hydrogen-rich conditions, however, near stoichiometric or even air-rich conditions could be used with reduced emission time delay and up to a factor of 4 reduced sensitivity. With increased air, the peak tail was more pronounced even at 150°C. Thus, in

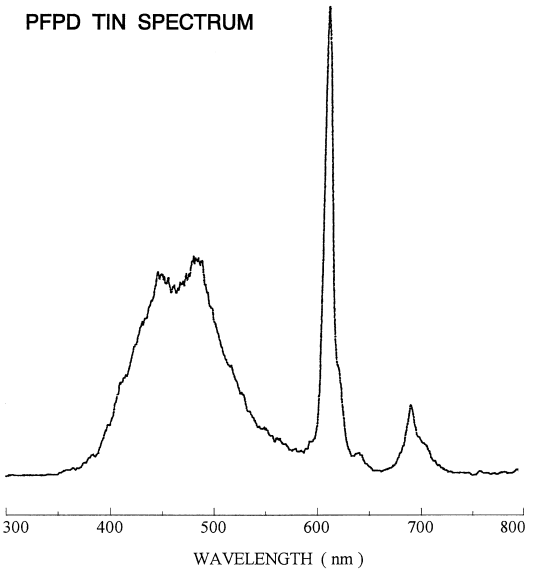

Fig. 11. PFPD time-delayed emission spectrum of tin. Tetraethyltin was introduced into the detector at 45°C. A WG360 filter was used at the entrance of the monochromator to suppress second-order dispersion.

order to eliminate other heteroatom interference, air-rich conditions at a PFPD temperature of about 350°C is recommended.

Tin peak tailing also existed with the FPD [9,19,20] when a quartz chimney was employed for enhanced sensitivity. With the PFPD it was reduced by increasing the base temperature to 350°C and also by increasing the gas flow and repetition rate to an acceptable level as shown in the chromatogram, in Fig. 13. On the other hand, when the PFPD was cooled to 150°C, the peak tailing was so long that an almost tail free GC peak was observed, with about three-times reduction in sensitivity. The penalty for this mode was that tin was accumulated (possibly on the combustor surface) and the total self cleaning took about 10 min. If there are several tin compounds, the baseline may progressively increase slightly.

We observed an MDL of 30 fg Sn/s with the limiting noise being twice the RMS noise. Using the reduced or tail free mode, the MDL was about 100 fg Sn/s. The selectivity against carbon was specific, but Sn detection was affected by S and P, depending on the combustor, filter, temperature and gas composition used.

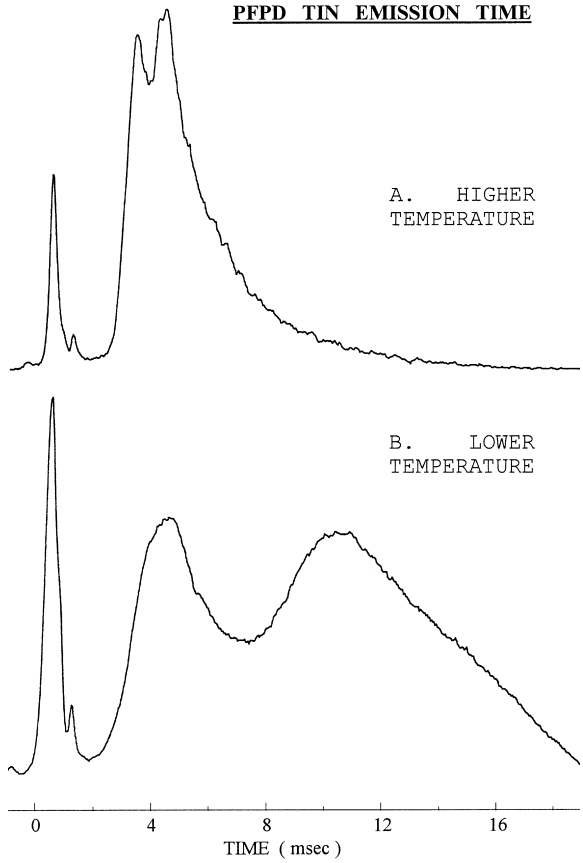

Fig. 12. Time dependence of tin emission in a pulsed flame. The PFPD base temperature was: (A) 350°C; (B) 180°C. A BG12 filter and R647 PMT were used.

Using a Varian PFPD, Jacobsen et al. [51] determined alkyltin compounds in sea water and environmental samples. Detection limits of 0.2 to 0.4 pg of the organotin compounds were observed and excellent long term stability has been reported.

3.1.5. Germanium

As shown in Fig. 14, germanium emission was dominated by twin peaks, at about 620 and 650 nm presumably due to germanium hydride [18]. A weaker band was also observed in the 400–500 nm range. Time-delayed emission was observed as shown in Fig. 15 which is similar but not identical to that of phosphorus, and results in a specific detection of germanium without any hydrocarbon interference.

A clean peak shape was obtained without peak

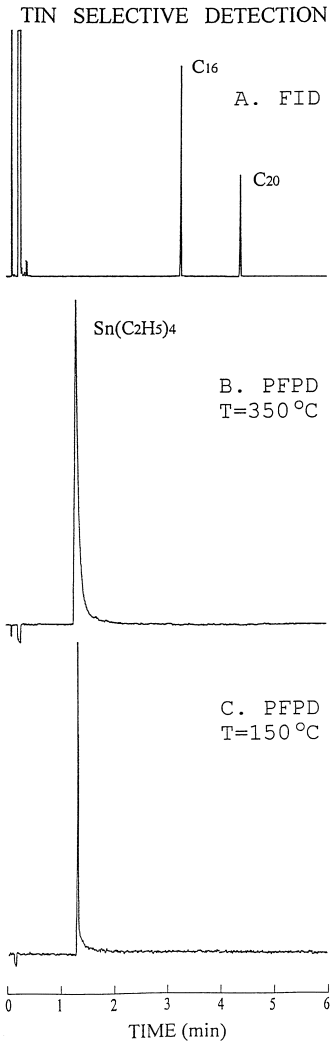

Fig. 13. Tin selective detection with the PFPD. 0.5 μl of a solution of $4 \cdot 10^{-6}$ tetraethyltin, 1% hexadecane and 0.5% eicosane was injected with a split ratio of 50:1. The column was kept at 60°C for 1 min and then ramped to 200°C (for 2 min) at 40°C/min. A BG12 filter and R647 PMT were used. The PFPD base temperatures were as shown in the Figure.

tailing as illustrated in Fig. 16. An OG590 filter was used combined with an R5070 red sensitive PMT. It can also be combined with the standard R647 with some small reduction in sensitivity. We did not use the intense surface chemiluminescence reported by Flinn and Aue [18]. A PFPD base temperature of 350°C enabled good long term stability but 200–300°C could also be used.

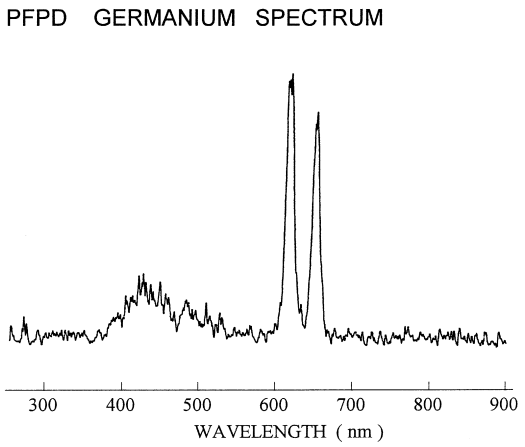

Fig. 14. PFPD time-delayed emission spectrum of germanium. Germanium(IV) methoxide was introduced into the PFPD at 50°C.

Dissociation in solution, syringe and the column should be monitored with $Ge(OCH_3)_4$ as it reacted immediately with water or ethanol due to ligand substitution. Thus, $Ge(C_2H_5)_4$ was eventually used.

3.1.6. Gallium

As shown in Fig. 17, the gallium flame emission spectrum was dominated by a strong line at 418 nm that was probably an atomic line. Another line at 568 nm was presumably due to gallium hydride and is

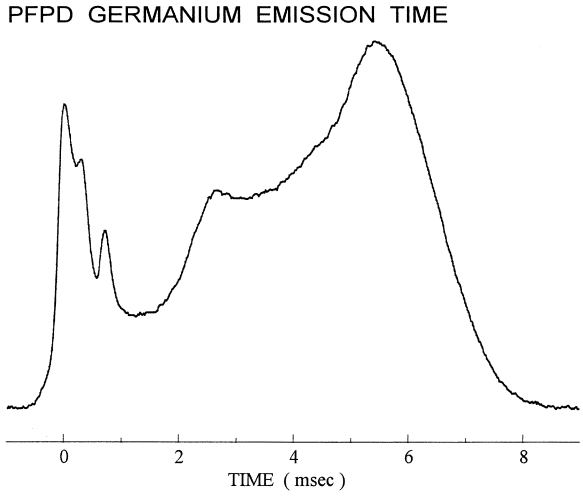

Fig. 15. Time dependence of germanium emission in a pulsed flame. The PFPD base temperature was 250°C. An OG590 filter and R5070 PMT were used.

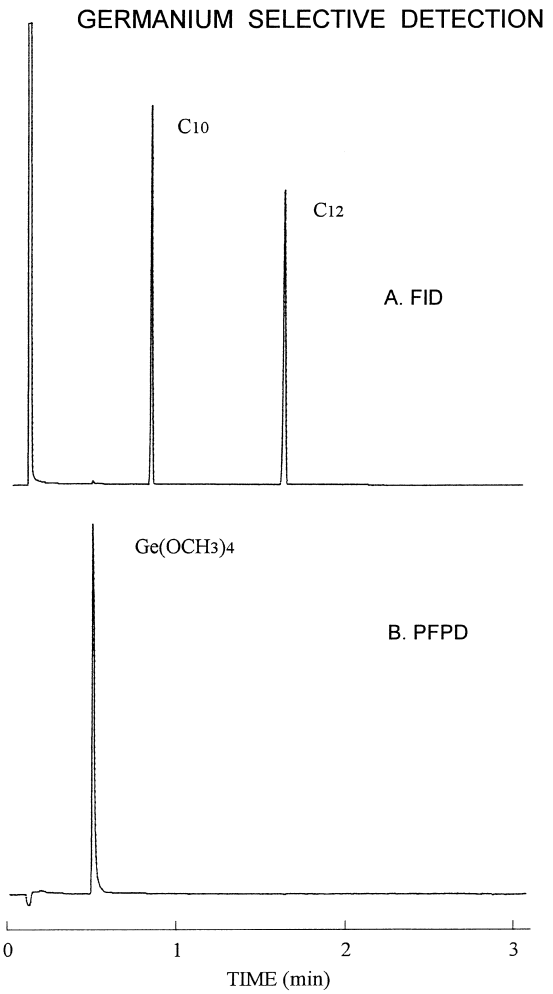

Fig. 16. Germanium selective detection with the PFPD. The injector temperature was 240°C. 0.5 μl of a methanol solution of $4 \cdot 10^{-4}$ tetramethoxygermanium, 1% decane and dodecane was injected with a split ratio of 120:1. The column temperature was ramped from 50 to 140°C at 30°C/min. The PFPD base temperature was 250°C, and an OG590 filter and R5070 PMT were used.

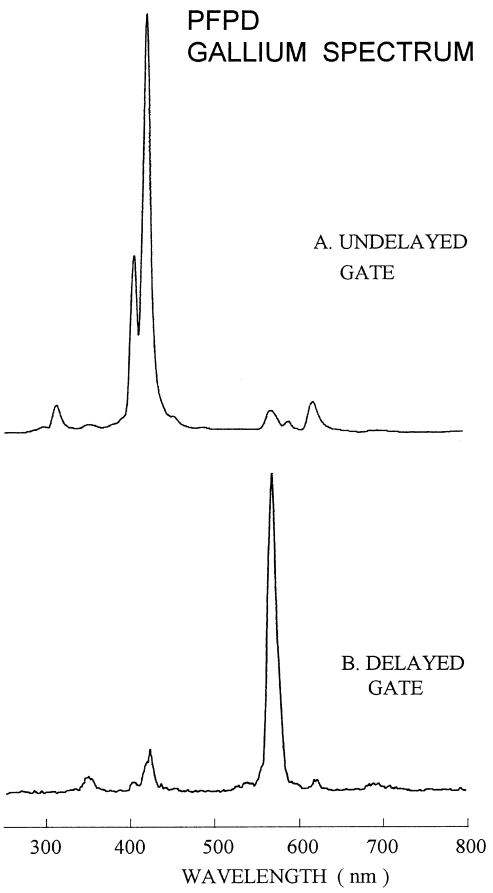

Fig. 17. PFPD time-delayed and undelayed emission spectra of gallium. Gallium(III) acetylacetonate was introduced into the PFPD at 185°C.

the most analytically important line due to its emission time delay.

Time-delayed emission of Ga is shown in Fig. 18. The optimal delay time was intermediate between that of phosphorus and sulfur. Due to its delayed emission, specific response was obtained in its selectivity against hydrocarbons. The best filter for Ga was an OG550 with an R647 PMT for observing all of the delayed light with minimal interference from other heteroatoms. Other filters can be used as long as they include the 568 nm range, or the 418 nm line under air-rich conditions with a undelayed gate.

A clean GC peak is demonstrated in Fig. 19 with a sensitivity of 1 pg Ga/s using a PFPD temperature of 200°C. We used gallium(III) acetylacetonate [$Ga(acac)_3$] which was found to be thermally labile, requiring a high column flow-rate, large split gas flow-rate and low PFPD temperature to reduce its decomposition at the detector base. Calibration of the sensitivity was done with the FID giving a correction factor of 4.5.

3.1.7. Antimony

Antimony can be selectively detected with the

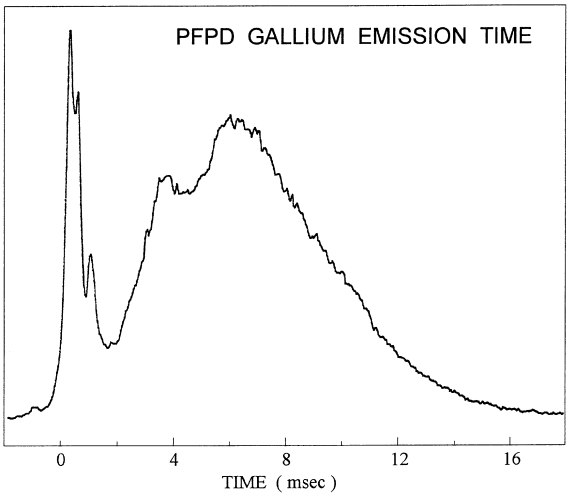

Fig. 18. Time dependence of gallium emission in a pulsed flame. An OG550 filter and R647 PMT were used with the PFPD. The PFPD base temperature was 200°C.

PFPD with relatively low sensitivity but with infinite selectivity against hydrocarbons.

In order to get the PFPD antimony emission spectrum, antimony(III) ethoxide was introduced into the PFPD from the tee inside the column oven. A large antimony sampling rate usually caused combustor coating problems that poisoned the combustor and considerably diminished its time-delayed emission. Since its emission was relatively weak and only a small amount of the antimony compound was introduced into the PFPD, poor S/N ratio was obtained as shown in Fig. 20. The small spectral peak at about 310 nm was from undelayed OH emission (due to a gate delay which was too short) and should be ignored. The delayed emission spectrum of antimony was very broad, from 450 nm up to the end of the red edge of the PMT limit, and was similar to that obtained with a conventional FPD [26]. Therefore, any filter above 450 nm could be used. Our choice was an OG590 filter with an R5070 PMT to reduce S and P emission as well as the pulsed flame background.

Time-delayed emission was observed for Sb that could be very long under hydrogen-rich conditions, as shown in Fig. 21, or with a short delay under close to stoichiometric conditions. Thus, specific detection could easily be obtained. Undelayed emission was also observed under air-rich conditions.

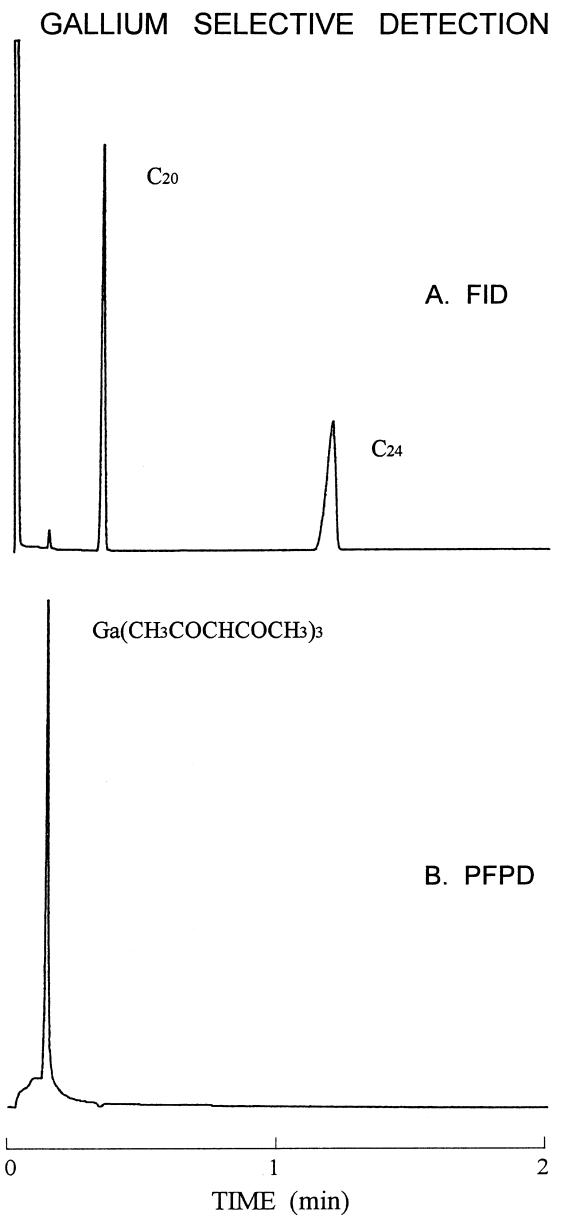

Fig. 19. Gallium selective detection with the PFPD. 0.9 μl of a solution of $6.6 \cdot 10^{-4}$ gallium(III) acetylacetonate, 1% eicosane and tetracosane was injected at 280°C with a split ratio of 40:1. A carrier gas flow-rate of 4 ml He/min was used. The column temperature was ramped from 180 to 200°C at 10°C/min. A 3 mm I.D. combustor, OG550 filter and R647 PMT were used. The PFPD base temperature was 200°C.

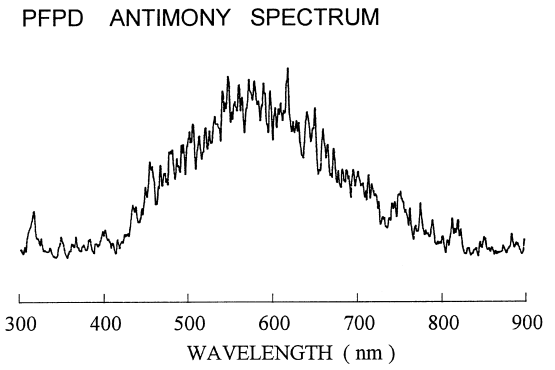

Fig. 20. PFPD time-delayed emission spectrum of antimony. Antimony(III) ethoxide was introduced into the PFPD at 150°C.

PFPD detection of Sb was optimized under hydrogen-rich gas composition, but was relatively insensitive to the gas composition. One could also work with only a small excess of hydrogen and a shorter delayed gate. A higher flow-rate of the combustible gas is recommended to reduce the peak tailing. Air-rich conditions could be used for better sensitivity with lower selectivity using undelayed emission detection.

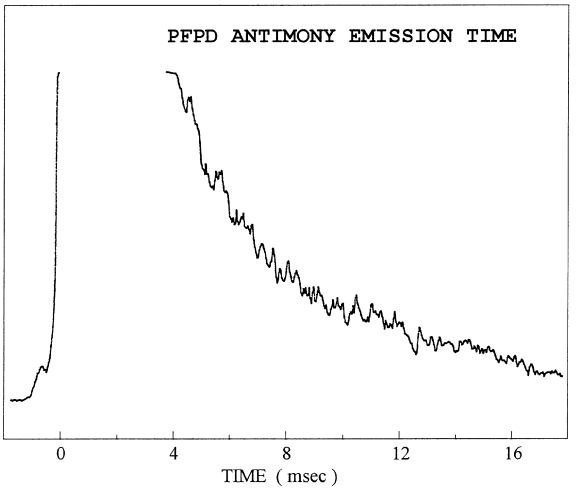

Fig. 21. Time dependence of antimony emission in a pulsed flame. An OG590 filter and R647 PMT were used with the PFPD. The delayed emission of antimony can be observed with all gas compositions ranging from very air-rich to normal hydrogen-rich. However, the richer the air content, the shorter the time delay. The emission at the main flame background position also contains undelayed emission of antimony, similar to arsenic emission in Fig. 5.

Poor peak shape with long tailing was observed even at high detector temperatures as shown in trace C of Fig. 22. Initially, when the detector was clean, a PFPD temperature of 200°C was sufficient, and no peak tailing was observed. Peak tailing developed in time and could not be removed except by cutting the

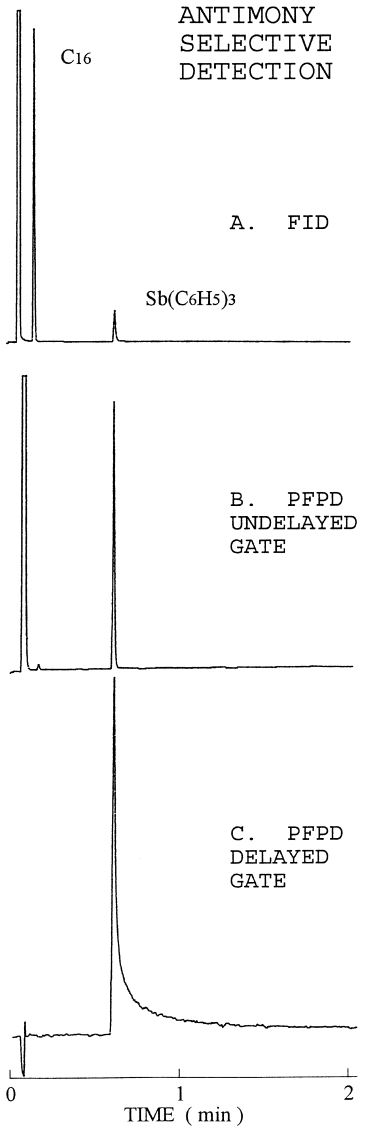

Fig. 22. Antimony selective detection with the PFPD. 0.5 μl of a toluene solution of 1% hexadecane and $1.5 \cdot 10^{-3}$ triphenylantimony was injected with a split ratio of 100:1. The column temperature was ramped from 190 to 250°C at 40°C/min. An OG590 filter and R5070 PMT were used for both B and C.

end of the column and by cleaning the combustor. When peak tailing appeared, a PFPD temperature of 350°C was required to reduce it and maintain steady state operational conditions. Under these conditions, 200°C could be employed with reduced tailing that was longer in time.

The MDL was obtained with a large uncertainty due to several problems. About 30 pg Sb/s was achieved with the R5070 PMT and OG590 filter for delayed gate operation with infinite Sb/C selectivity. An air-rich gas composition with undelayed emission resulted in an MDL of 3 pg Sb/s and an Sb/C selectivity of 1000. With the R647 PMT and GG495 filter the MDL was about two-times greater. An approximately linear response was observed, with a low linear dynamic range of ~30 due to limited sensitivity and self quenching at high concentrations.

Antimony(III) ethoxide, $Sb(OC_2H_5)_3$, was initially used as the source compound. However, it was very sensitive to water, and also rapidly reacted with solvents such as methanol, while it did not dissolve in toluene or octane. Upon solvation with an alcohol other than ethanol, a rapid ligand exchange occurred so we used ethanol. A considerable amount of sample was lost due to ~0.2% water in the solvent, thus FID calibration was essential since the solution degraded with time. A gradual and irreversible peak tailing developed in time due to the large amount of antimony compound used as a result of its low sensitivity. Triphenylantimony, $Sb(C_6H_5)_3$, was also used. Although it was better than $Sb(OC_2H_5)_3$, it also developed peak tailing problems in time.

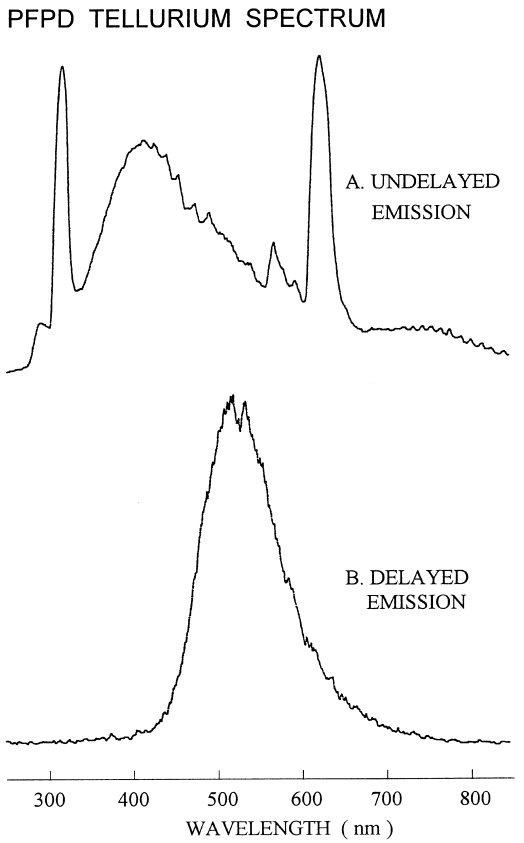

Fig. 23. PFPD time-delayed and undelayed emission spectra of tellurium. Diphenylditelluride was introduced into the PFPD at about 170°C. The OH emission band (~310 nm) and its second-order (~620 nm) should be ignored whereas the small maximum around 570 nm might be from background residue. A 2 mm I.D. combustor was used.

3.1.8. Tellurium

As shown in Fig. 23, tellurium exhibited two types of emission: (a) a broad, structureless and delayed emission from 450 to 600 nm, probably emerging from Te_2 (similar to S_2 or Se_2) and resulting in a quadratic response; (b) a blue undelayed emission from 340 to 500 nm, probably from TeO under slightly air-rich conditions, which, unlike the delayed one, was linear with the Te concentration.

As shown in Fig. 24, a long delayed emission was observed with the PFPD under hydrogen-rich conditions while a stronger undelayed emission was observed under air-rich conditions. Therefore, either a delayed gate under hydrogen-rich conditions for lower sensitivity and total selectivity or an undelayed gate with slightly air-rich conditions for higher sensitivity and lower selectivity was adopted. The filter used for the selective delayed gate mode was GG495 while BG12 or WG345 filters were used for the linear detection mode.

As demonstrated in Fig. 25, a clean GC peak shape was observed under both modes. However, a minor tail was encountered with the delayed emission under hydrogen-rich conditions. A 2 mm I.D. combustor was used for the hydrogen-rich, delayed gate mode (Te_2 detection), while a 3 mm I.D. combustor was presumably better with the air-rich, linear mode.

The undelayed gate mode of operation enabled the linear response under air-rich conditions, while the

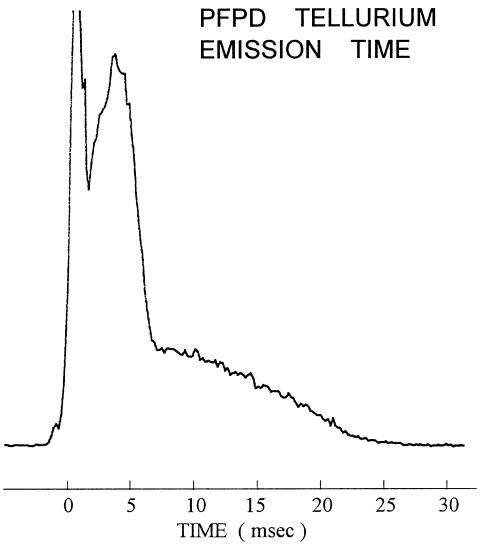

Fig. 24. Time dependence of tellurium emission in a pulsed flame. A GG495 filter and R647 PMT were used with the PFPD.

quadratic response dependence held for the delayed emission under hydrogen-rich conditions (tested for a small concentration range only). The delayed emission of Te_2 offered a specific response, but the Te/C selectivity in the air-rich, undelayed mode was limited to 150. The MDL was 200 pg Te/s with the quadratic delayed emission, and 3 pg Te/s in the linear, air-rich, undelayed mode. We used a PFPD base temperature of 220°C. Above 250°C some decomposition and sensitivity reduction was observed in the delayed mode.

3.1.9. Bromine

Bromine can be selectively detected with the PFPD with infinite selectivity but with poor sensitivity. The selectivity is also very good against Cl and F and is acceptable against I.

Fig. 26 shows the delayed emission of bromine. Thus, there is a specific response of bromine against carbon, chlorine and fluorine but not against sulfur, phosphorus and nitrogen.

Fig. 27 shows the chromatograms of bromobenzene and 2-bromotoluene together with chlorobenzene, 1,3,5-trichlorobenzene, 2-iodotoluene and 1-iododecane obtained with both the PFPD and the FID. Hydrogen-rich gas composition and a 2 mm I.D. combustor were used. An RG9 filter with R5070

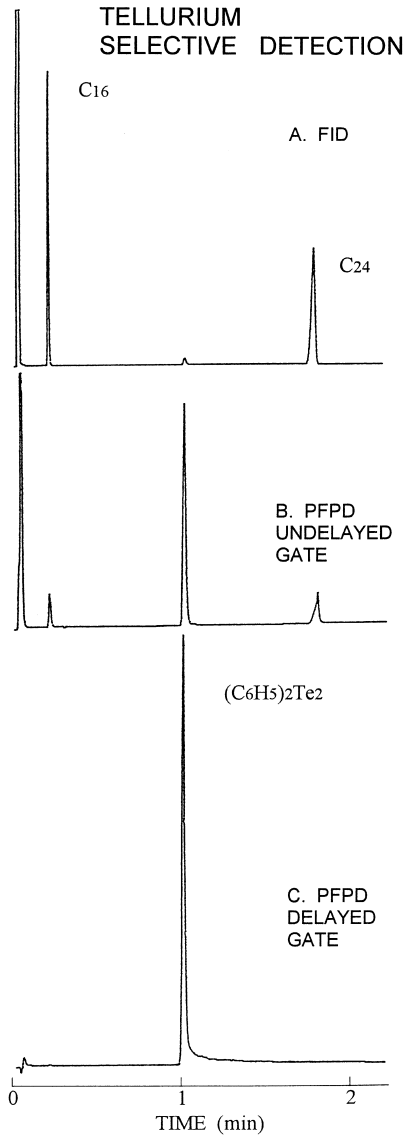

Fig. 25. Tellurium selective detection with the PFPD. 0.9 μl of a toluene solution of $3 \cdot 10^{-4}$ diphenylditelluride, $3 \cdot 10^{-3}$ hexadecane and tetracosane was injected with a split ratio of 30:1. A 3 m column was kept at 150°C for 0.3 min and then ramped to 210°C at 30°C/min. A BG12 filter (trace B) or GG495 filter (trace C) and R647 PMT were used with the PFPD. The PFPD base temperature was 220°C.

photomultiplier was used for detection above 735 nm. It is apparent that except for the two minor peaks corresponding to the iodine compounds, the PFPD is specific for bromine, and no detector

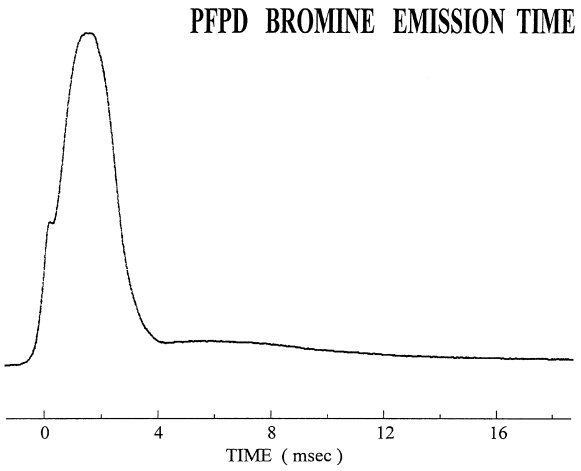

Fig. 26. Time dependence of bromine emission in a pulsed flame. An RG9 filter and R5070 PMT were used with the PFPD. Bromobenzene was used as the bromine source.

problems such as peak tailing occurred. However, the sensitivity was poor, and the MDL was 1 ng Br/s. A non-linear dependence was observed that began with an approximately quadratic dependence at the low nanogram Br/s level.

3.1.10. Copper

Copper can be detected with the PFPD with infinite selectivity against hydrocarbons.

As shown in Fig. 28, the emission spectrum of copper was structured and covered the entire 400–700 nm spectral range. The spectrum contained a band at 430 nm and atomic lines around 320–330 nm that resulted from undelayed emission (trace A), a band at 610–700 nm (presumably due to CuH) which was maximized under hydrogen-rich conditions (trace B), and a band at 500–600 nm. This band was the dominant emission under air-rich conditions (trace C) and was probably due to CuO, the band responsible for the Beilstein test for organohalide compounds through the vaporization of Cu induced by halogen atoms. Cu was also detected with the FPD at 327.4 nm by Hill and Aue [52].

The delayed emission of Cu, as shown in Fig. 29, was observed under both hydrogen-rich conditions, at the 610–700 nm spectral range, and air-rich conditions at the 510–600 nm band. Therefore, infinite selectivity against hydrocarbons was enabled with a delayed gate. The preferred detection mode is

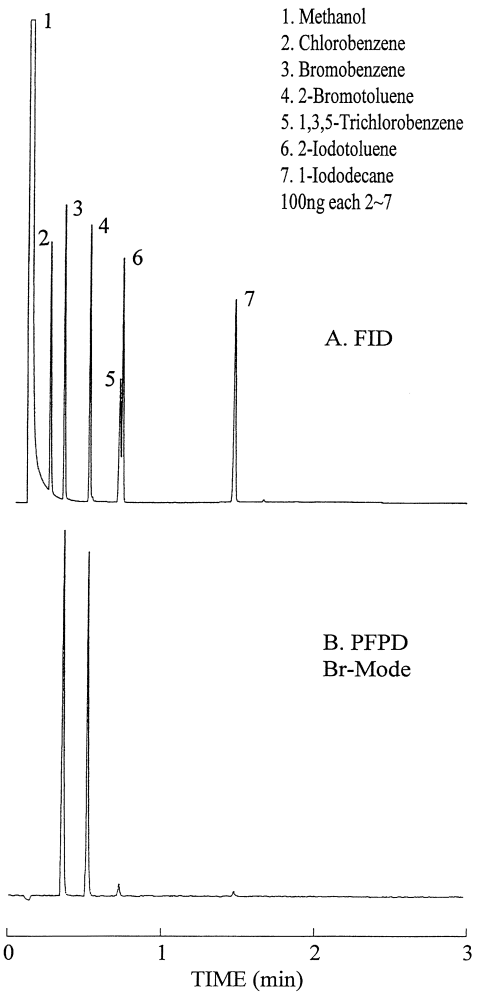

Fig. 27. Bromine selective detection with the PFPD. One μl of a methanol solution of $3 \cdot 10^{-3}$ chlorobenzene, 1,3,5-trichlorobenzene, bromobenzene, 2-bromotoluene, 2-iodotoluene and 1-iododecane was injected with a split ratio of 30:1. The column was temperature programmed from 70 to 150°C at 50°C/min. An RG9 filter and R5070 PMT were used. The PFPD base temperature was 200°C.

with a hydrogen-rich gas composition and delayed gate using a red sensitive PMT such as R1463 or R5070. Depending on the PFPD gas composition, an OG590 filter can be used under hydrogen-rich conditions. Alternatively, a GG495 filter can be used with R647 under air-rich conditions, but with lower sensitivity. A PFPD temperature of 280°C was used.

Clean chromatographic peak shape for Cu selective detection with the PFPD can be obtained, as

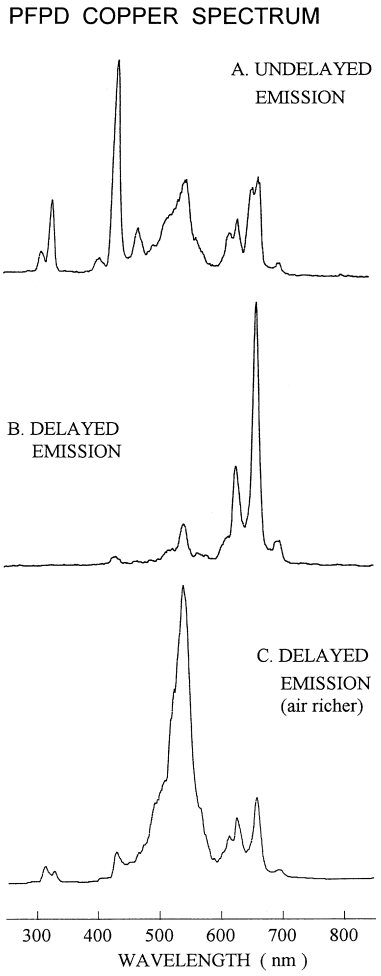

Fig. 28. PFPD time-delayed and undelayed emission spectra of copper. Copper(II) acetylacetonate was introduced into the PFPD at 165°C.

shown in Fig. 30. However, peak tailing could emerge due to the dissociation of copper(II) acetylacetonate at the column portion near the detector base. The Cu detection sensitivity was 4 pg Cu/s.

3.1.11. Indium

Indium was extensively tested for indium sensitized halogen selective detection. Indium metal itself exhibited two delayed emission bands near 600 nm (probably due to its hydrides) [31] that could serve for its selective detection. No GC experiment was performed due to the lack of organoindium compounds.

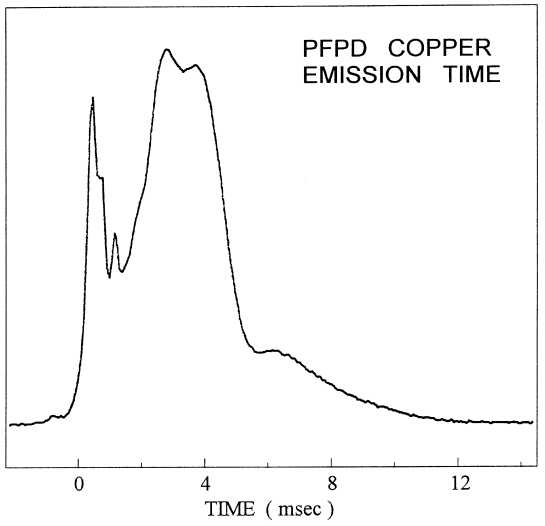

Fig. 29. Time dependence of copper emission in a pulsed flame. An RG645 filter and R5070 PMT were used with the PFPD.

3.2. PFPD detection of metal elements with undelayed emissions

With the exception of Pb, Bi and Al, all of the metal elements studied were transition metals. No time-delayed emission, on the millisecond time scale, was observed for any of these under our experimental conditions (some of these conditions are listed in Table 1). Regarding their sensitivities and selectivities relative to hydrocarbons, the best PFPD elements were Mn, Fe, Ru and Rh. The preferred pulsed flame gas composition was near stoichiometric or slightly air-rich, in contrast to that applied for the elements with time-delayed emissions discussed above. Atomic lines emerged in the emission spectra of some of these transition metals and thus a higher flame temperature was preferred. A careful emission time analysis performed with a smaller observation window revealed a small, approximately 0.5 ms delay in the emission of atomic lines that depended on the peak pulsed flame temperature. This short delay was insufficient for analytical usage under our standard conditions and thus was not further explored. A PFPD base temperature of 300°C was usually used unless otherwise indicated. Since the undelayed emission of these elements was not separated in time from the pulsed flame background or from hydrocarbon emissions, the second-order

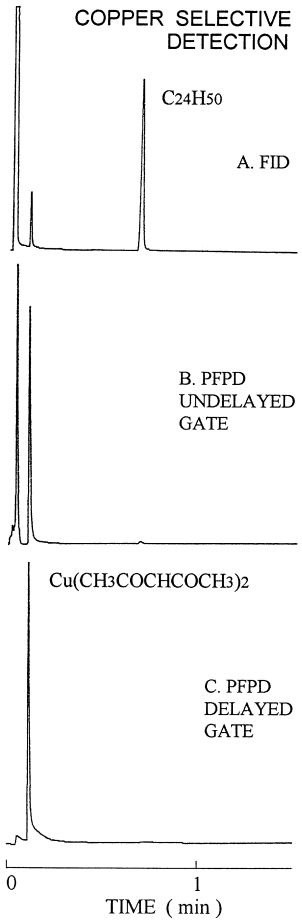

Fig. 30. Copper selective detection with the PFPD. One μl of a solution of $7 \cdot 10^{-4}$ copper(II) acetylacetonate and $1 \cdot 10^{-3}$ tetracosane was injected with a split ratio of 40:1. The column temperature program was from 190 to 240°C at 30°C/min. An R647 PMT with a GG495 filter, and R5070 with an RG645 filter were used in B and C, respectively. The PFPD base temperature was 280°C.

dispersion of the flame background (OH) in the monochromator occurred in the spectra of certain elements, such as Cr, Ru and Ni.

We observed that a detector self-cleaning mechanism existed in the PFPD, which was due to the quartz combustor used and its direct contact with the pulsed flame. This is in contrast to the optical window of FPD that can be irreversibly covered with non-volatile flame products such as metal oxides. When a heteroatom compound produced a GC peak with peak tailing, the tail could last a relatively short time, or longer time with much lower amplitude. For example, when a solution of ferrocene was injected while a constant sulfur background was introduced, we found that the iron quenched the sulfur delayed emission, but this emission recovered after less than a minute. This implies that iron does coat the combustor, but only for a short time, and is sufficient to quench delayed emission if it exists.

In this section, we describe these metal elements (with the exception of Ru and Rh) roughly according to the order of detection sensitivity decline with the PFPD.

3.2.1. Manganese

Manganese can be selectively detected with the PFPD with high selectivity against hydrocarbons. The PFPD can be used successfully for the detection of the fuel additive methylcyclopentadienyl manganese tricarbonyl (MMT) in gasoline.

As can be seen from Fig. 31, the emission spectrum of Mn is dominated by the Mn atomic line at 403 nm. Several other lines and weak emission

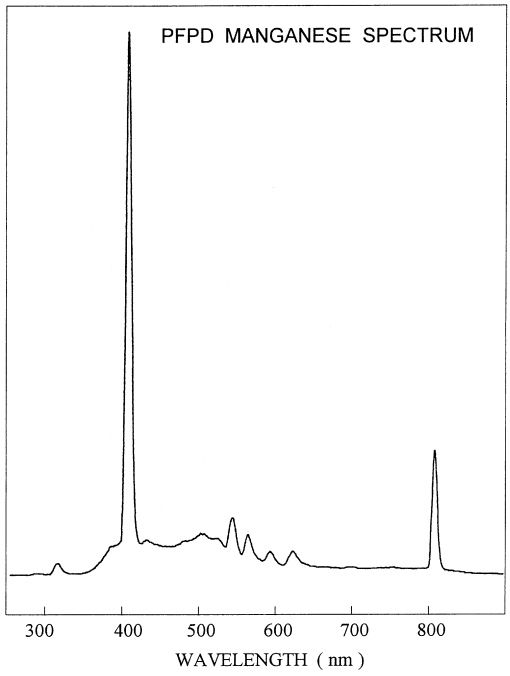

Fig. 31. PFPD undelayed emission spectrum of manganese. Manganese was introduced into the PFPD as methylcyclopentadienyl manganese tricarbonyl at 40°C. The peak at about 806 nm was the second-order of the Mn atomic line, at 403 nm.

peaks are observed in the 380–600 nm range. Therefore, the best selectivity of manganese was achieved with an interference filter. An Andover 405FS10-25 interference filter with a 10 nm band width was used. A WG345 filter can also be used albeit with 3–4 times lower selectivity and about the same MDL. With the interference filter, the triggering early light spike was relatively weak and triggering was done on the main flame background.

Slightly air-rich conditions (near stoichiometric conditions) were preferred for manganese detection to maximize the pulsed flame temperature and thus the atomic line emission. The optimum was not sensitive to the exact gas composition which could be set according to the required selectivity against other elements. A 3 mm I.D. combustor was preferred, the response being twice that observed with a 2 mm I.D. combustor.

As shown in Fig. 32, a clean GC peak of MMT was observed with a long tail that could be up to 5% of the height. The magnitude of the tail portion depended on the gas composition, and was minimized under near stoichiometric conditions, while under H_2-rich conditions a slight derivatization could be observed. At a lower PFPD temperature of 200–250°C this tail disappeared, and self cleaning occurred in about 5–10 min. The PFPD temperature was relatively unimportant except that at or below 200°C no peak tailing was observed.

With an Andover 405FS10-25 interference filter having a 10 nm band width, the Mn/C selectivity was $1.2 \cdot 10^4$ while with BG12 it was about $3 \cdot 10^3$. The MDL of manganese detection was around 100 fg Mn/s with both filters as above.

Fig. 33 shows the analysis of manganese in gasoline spiked with 30 ppm of MMT. The Figure demonstrates compatibility with the analysis requirement of this fuel additive used in Canada [28] and elsewhere [12]. The detection of MMT additive in gasoline using a conventional FPD was reported by Aue et al. [28]. In our experiment, a 4-m narrow bore column was found to be sufficient to separate the MMT from all the hydrocarbons within 4 min. While the maximum MMT allowed level is 80 ppm [28], 30 ppm was detected with very good S/N and no interference. We used near stoichiometric gas composition at a PFPD temperature of 210°C, and an interference filter at 405 nm with an R647 PMT. The injected amount was 0.8 μl with a split ratio of 100 so that 8 μg were analyzed. The low sample volume was desirable to totally eliminate sulfur interference that was further suppressed under the air-rich gas composition and with an undelayed gate.

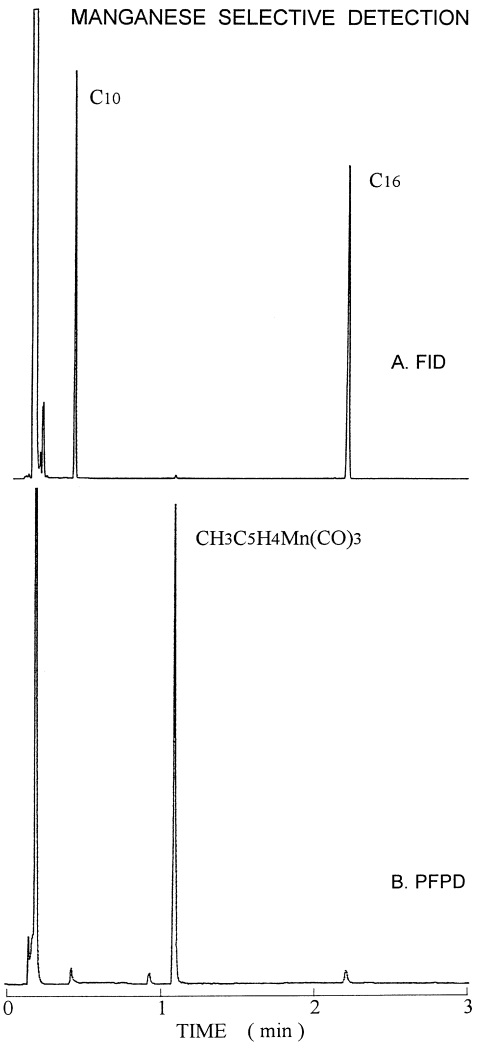

Fig. 32. Manganese selective detection with the PFPD. At an injector temperature of 250°C, 75 pg of Mn was injected as methylcyclopentadienyl manganese tricarbonyl together with 30 ng decane and hexadecane. The column temperature was kept at 80°C for 0.5 min, and then ramped to 200°C at 40°C/min. An undelayed 7 ms gate was used. An Andover 405 FS10-25 interference filter was used with an R647 PMT. The PFPD base temperature was 200°C.

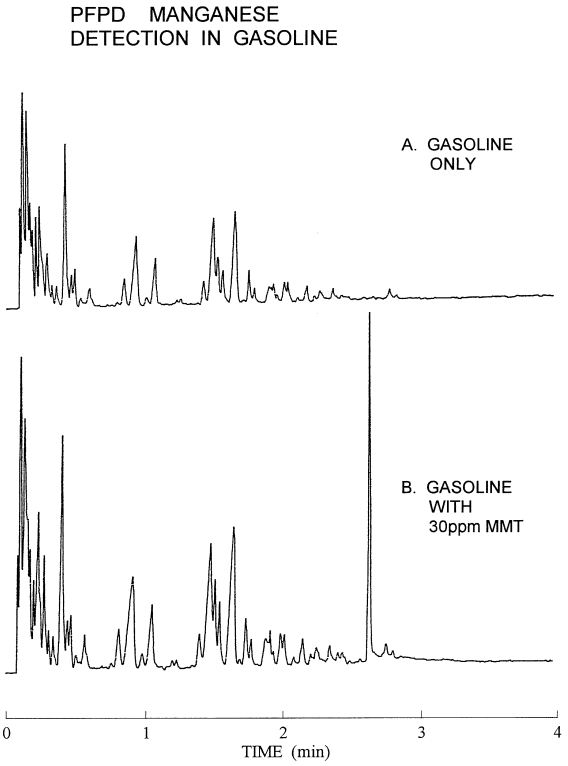

Fig. 33. Analysis of a manganese additive in gasoline with the PFPD. Unleaded Gasoline 91 octane was spiked to contain $3 \cdot 10^{-5}$ methylcyclopentadienyl manganese tricarbonyl. 0.8 μl was injected with a split ratio of 100:1. The column temperature was kept at 40°C for 1 min, and then ramped to 160°C at 40°C/min. An undelayed gate was used and an Andover 405 FS10-25 interference filter was used with an R647 PMT.

3.2.2. Iron

Iron selective detection with conventional FPDs has been extensively studied [1,15,21,52,53]. With the PFPD, iron can be selectively detected with relatively high selectivity. A broad flame emission spectrum, which is rich in structure, is observed from 360 nm to 800 nm as shown in Fig. 34. The bands at 360–400 nm and 680–800 probably contain the atomic lines of Fe, while the 470–630 nm spectral range is enhanced in the air-rich flame. A GG495 filter was used as it proved to have the best selectivity to reduce carbon emission. Similar sensitivity was observed with the WG345 filter with a selectivity reduction factor of about 2. Using the OG590 enabled further increased selectivity with a factor of

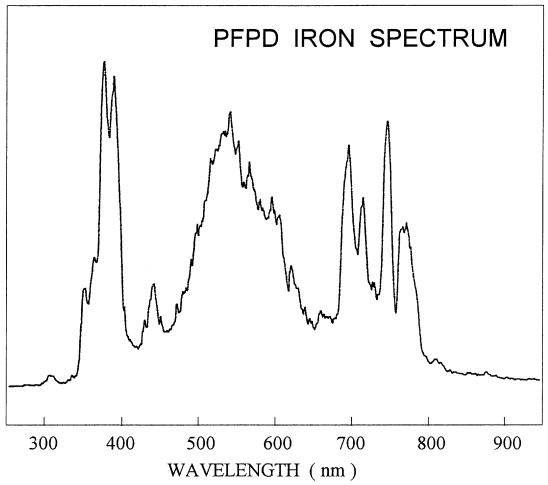

Fig. 34. PFPD undelayed emission spectrum of iron. Ferrocene was introduced into the PFPD at 100°C.

2 sensitivity loss. The MDL was 0.3 pg Fe/s, while the Fe/C selectivity was 2000 with the GG495 filter.

Ferrocene was used and found to be a stable compound for the study. A clean GC peak shape is demonstrated in Fig. 35.

3.2.3. Chromium

Chromium has also been extensively studied with conventional FPDs [1,3,4,29,30,54]. With the PFPD, chromium can be selectively detected with medium selectivity.

As shown in Fig. 36, an unresolved structure from 350–800 nm was observed together with several lines. The line at 428 nm was the strongest and was probably an atomic line. A GG495 filter was found to be optimal, but an interference filter around 428 nm can be used for better Cr/C selectivity if it is separated from the nearby 432 nm CH band.

As shown in Fig. 37, clean peak shape was observed, followed by a low ~2% long tail that recovered after a few minutes.

3.2.4. Ruthenium

Ruthenium was found [22,25,29] to be the most sensitive transition metal element for FPD detection. Ruthenium was selectively detected with the PFPD

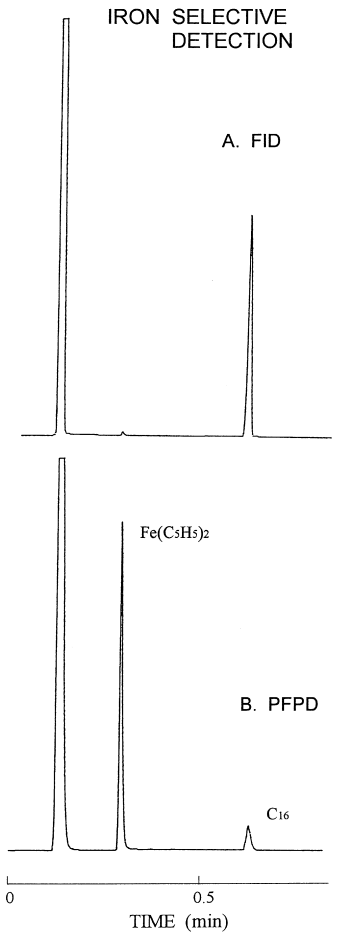

Fig. 35. Iron selective detection with the PFPD. 0.5 μl of a toluene solution of $1.4 \cdot 10^{-4}$ ferrocene and 1% hexadecane was injected with a split ratio of 120:1. The column temperature was ramped from 140 to 190°C at 30°C/min. An R647 PMT and GG495 filter were used with the PFPD. The PFPD base temperature was 300°C.

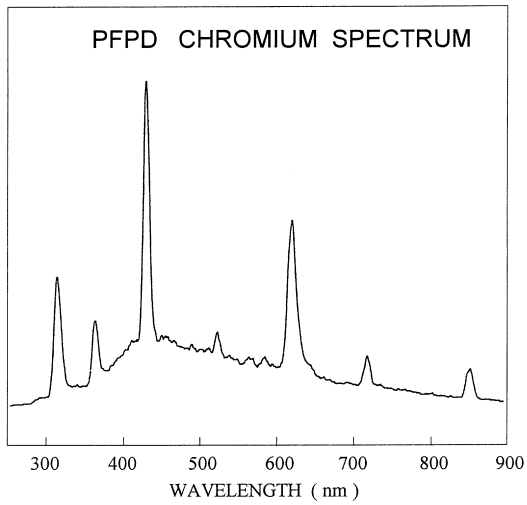

Fig. 36. PFPD undelayed emission spectrum of chromium. Chromium(III) acetylacetonate was introduced into the PFPD at 140°C.

with very high selectivity although very few of its compounds are amenable for GC separation.

As shown in Fig. 38, a structured emission spectrum was observed which is superimposed on a continuum background covering the entire visible range of 350–800 nm. Both ruthenocene and $Ru_3(CO)_{12}$ were used and identical spectra were obtained for each. We used either GG495 filter with R647 PMT or OG590 filter with R5070 PMT for further improved selectivity.

As shown in Fig. 39 the GC peak shape was quite clean but with a minor peak tail. A PFPD temperature of 350°C was used to reduce the small peak tail.

3.2.5. Rhodium

Rhodium can be selectively detected with the PFPD with high selectivity. However, it creates problems through the promotion of catalytic combustion by its presence on the combustor. We were unable to obtain a spectrum due to the catalytic combustion problem, but Rh has been detected by Juvet and co-workers [1,3,4] using their laboratory-built FPD with 369 nm wavelength detection (its strongest atomic line). Due to this adverse catalytic effect, one must wait between injections and restrict the injected amount.

The GC peak shape was clean as shown in Fig. 40. We used rhodium(III) acetylacetonate, with a GG495 filter and R647 PMT for improved selectivity.

3.2.6. Europium

As shown in Fig. 41, europium exhibits a strong structured emission band in the 590–710 nm spectral range. The single band at about 460 nm probably originates from its atomic lines. Based on the observed spectrum, we only used the OG590 filter with R1463 PMT.

For optimal sensitivity the adjusting needle-valve

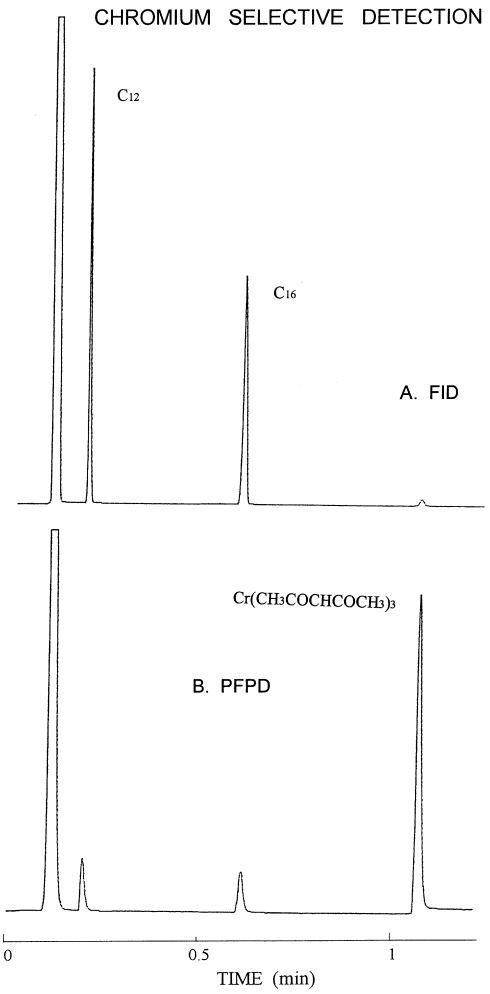

Fig. 37. Chromium selective detection with the PFPD. 0.5 μl of a toluene solution of $9 \cdot 10^{-4}$ chromium(III) acetylacetonate and 1% dodecane and hexadecane was injected with a split ratio of 100:1. The column temperature was ramped from 140 to 180°C at 30°C/min. An R647 PMT and GG495 filter were used with the PFPD. The PFPD base temperature was 300°C.

should be positioned further away from the ''tic-tock'' [45] pulsed flame conditions to reduce water in the combustor. A PFPD temperature of 280°C was used.

As shown in Fig. 42, GC peak tailing was observed both in the PFPD and FID in addition to column losses of the Eu compound. We assumed that this originated from the column and not the PFPD. The MDL was around 1 pg Eu/s with an Eu/C

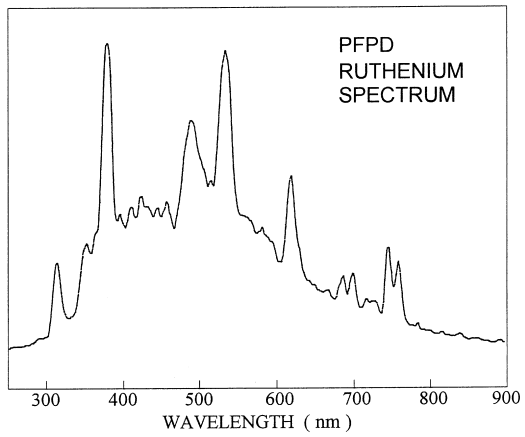

Fig. 38. PFPD undelayed emission spectrum of ruthenium. Ruthenocene was introduced into the PFPD at 100°C. The same spectrum was also obtained with $Ru_3(CO)_{12}$ introduced at 200°C.

selectivity of 10^4. Due to column losses, the FID calibration was not very reliable. Tris(2,2,6,6-tetramethyl-3,5-heptanedionato)europium, $[(CH_3)_3CCO\text{-}CH{=}C(O\text{–})C(CH_3)_3]_3Eu$, was a highly thermally labile compound that required a high flow-rate (5 ml/min), narrow bore, thin film, short column and attention to column losses. Linear response was thus obtained on a narrow range due to column and injector trapping problems. Several injections were needed to arrive at a steady state.

Other rare earth elements might be similarly detected with the PFPD if their organic compounds are amenable for GC separation.

3.2.7. Nickel

Nickel can be selectively detected with the PFPD with medium selectivity. It can be seen from Fig. 43 that Ni showed a sharp strong band at about 351 nm (presumably from its atomic lines), which appeared to be much weaker in a conventional FPD [29] and a structured broad band in the 500–750 nm range. A slightly air-rich gas composition was optimal for the atomic lines. The GG495 filter was optimal for selectivity, but an interference filter at 351 nm also seems to be suitable (not tested).

A clean peak shape is shown in Fig. 44 for the selective determination of Ni against C. The sensitivity was 1 pg Ni/s, and the Ni/C selectivity was 500 with the GG495 filter.

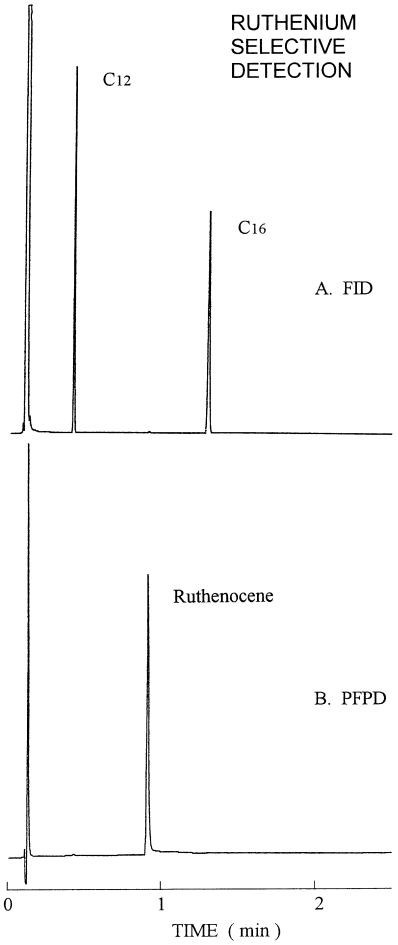

Fig. 39. Ruthenium selective detection with the PFPD. 0.5 μl of a toluene solution of $2.8 \cdot 10^{-5}$ ruthenocene and 0.3% dodecane and hexadecane was injected with a split ratio of 100:1. The column temperature was ramped from 100 to 200°C at 40°C/min. An R5070 PMT and OG590 filter were used with the PFPD. The PFPD base temperature was 350°C.

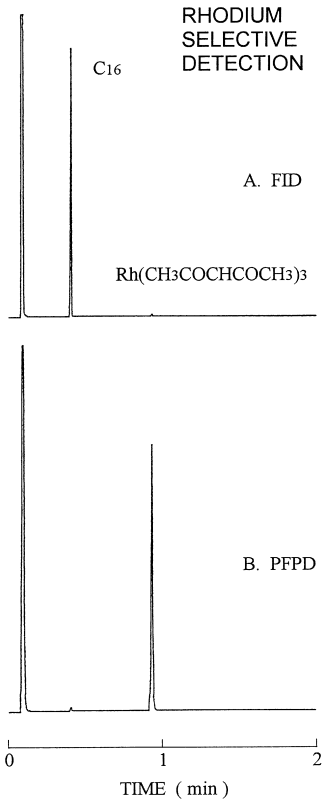

Fig. 40. Rhodium selective detection with the PFPD. 0.5 μl of a 2,4-pentanedione solution of $4.7 \cdot 10^{-4}$ rhodium(III) acetylacetonate and 1% hexadecane was injected with a split ratio of 100:1. The column temperature was ramped from 150 to 210°C at 50°C/min. An R647 PMT and GG495 filter were used with the PFPD. The PFPD base temperature was 300°C.

Nickelocene was used for this study and was found to be stable in toluene but decomposed in methanol and ethanol.

3.2.8. Vanadium

Vanadium was found [25] to be an element with no significant FPD response. However, our study shows that vanadium can be selectively detected with the PFPD with high selectivity. Shown in Fig. 45 is the spectrally broad emission of vanadium ranging from 350 to 900 nm, in which several atomic lines are presumably contained between 520 and 800 nm. Thus, an OG590 filter with R1463 PMT was chosen to be the best.

Clean peak shape for the selective detection of V is shown in Fig. 46. A PFPD temperature of 320°C was used.

The MDL obtained was 2 pg V/s with the OG590 filter, and 5 pg V/s with the RG9 filter. The V/C selectivity was 3000 with the OG590, and 8000 with the RG9 filter.

3.2.9. Tungsten

Tungsten was also found [25] to be one of the elements with no significant response in a conventional FPD, although earlier work [4] demonstrated good FPD detectability with both selective and

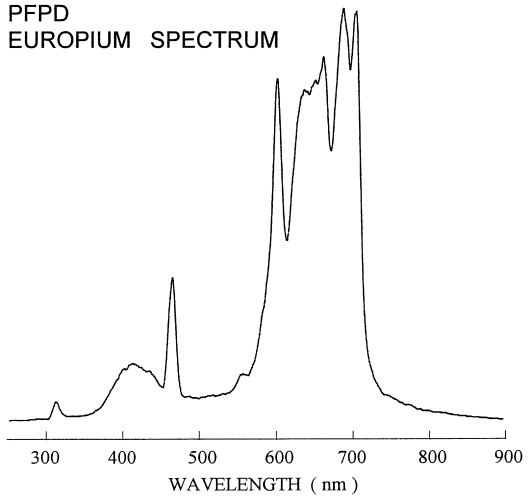

Fig. 41. PFPD undelayed emission spectrum of europium. Tris(2,2,6,6-tetramethyl-3,5-heptanedionato)europium was introduced into the PFPD at 160°C.

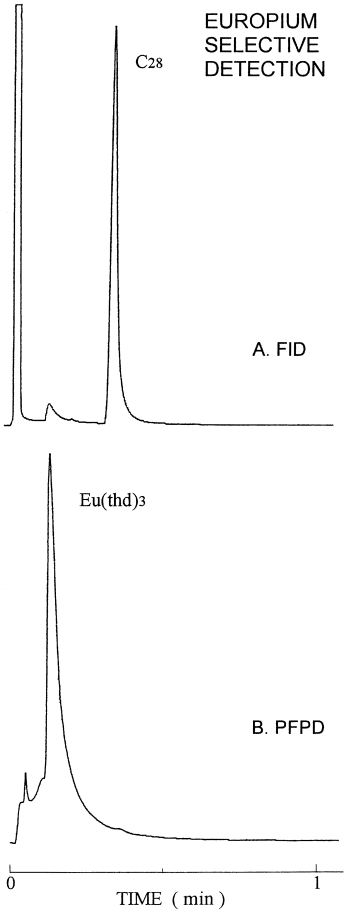

Fig. 42. Europium selective detection with the PFPD. 0.9 μl of a toluene solution of $4.7 \cdot 10^{-4}$ tris(2,2,6,6-tetramethyl-3,5-heptanedionato)europium, [$Eu(thd)_3$], and $4 \cdot 10^{-3}$ octacosane was injected with a split ratio of 30:1. The column was maintained isothermally at 235°C, with 5 ml/min He carrier gas flow-rate. An R1463 PMT and OG590 filter were used with the PFPD. The PFPD base temperature was 250°C.

nonselective modes. Our experiment shows that tungsten can be selectively detected with the PFPD with medium selectivity. As shown in Fig. 47 a structureless emission band was observed through the whole visible range of 400–800 nm. We used a GG495 filter, but other filters could be used.

Clean peak shape was observed for selective detection of W as shown in Fig. 48. The MDL was around 2 pg W/s. The calculated W/C selectivity was 740 and involved no FID calibration since $W(CO)_6$ was considered to have no FID response. A PFPD temperature of 280°C was used. A red sensitive R5070 PMT with an OG550 filter allowed enhanced selectivity with a small penalty in sensitivity.

3.2.10. Aluminum

Aluminum can be selectively detected with the PFPD with medium selectivity. As shown in Fig. 49, a broad emission spectrum was observed with a few lines in the 380–700 nm spectral range. The maximum occurred at a wavelength of 486 nm, which was due to the aluminum oxide emission band and has been used by Zado and Juvet [4] for the detection of Al with a FPD.

Clean peak shape was obtained for the PFPD detection of Al as shown in Fig. 50. A GG495 filter with R647 PMT, and PFPD temperature of 320°C were used.

3.2.11. Lead

In a conventional FPD, lead does not show the elemental flame emission lines at 405.8 nm and near 370 nm but rather several other weak bands in the spectral range 400–700 nm [26]. We found that lead could be detected with the PFPD with medium–low sensitivity and selectivity that could be useful in combination with GC separation. The best filter for

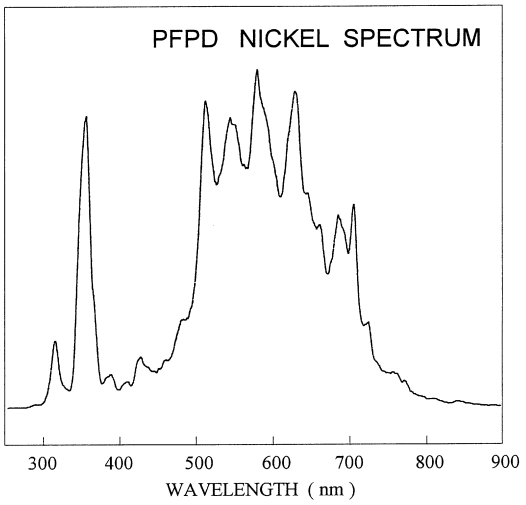

Fig. 43. PFPD undelayed emission spectrum of nickel. Nickelocene was introduced into the PFPD at 70°C.

lead detection with the PFPD was BG12. Unlike with the FPD, the atomic lead emission lines were observed with the PFPD (not shown), but they were relatively weak. The use of an interference filter centered around 405 nm did not improve the selectivity, but reduced the sensitivity by a factor of about 2.6 due to exclusion of other bands.

Fig. 51 shows the detection of lead with the PFPD with no peak tailing. The MDL obtained was 10 pg Pb/s with the limiting noise being twice the RMS noise, which is much better than that obtained with a commercial FPD [15]. A PFPD temperature of 350°C is recommended for tetraphenyllead. However, with other more volatile compounds a lower temperature can be used. A 3 mm I.D. combustor yielded a 1.9-times higher response than a 2 mm I.D. combustor. We measured a Pb/C selectivity of 80 with the BG12 filter.

Due to its limited selectivity the PFPD probably cannot be employed for the selective detection of lead in gasoline, except when a good chromatographic separation is achieved.

3.2.12. Bismuth

Bismuth can be detected with the PFPD with low sensitivity and limited Bi/C selectivity.

Insufficient data was obtained for the emission spectrum due to the low emission intensity of Bi, but

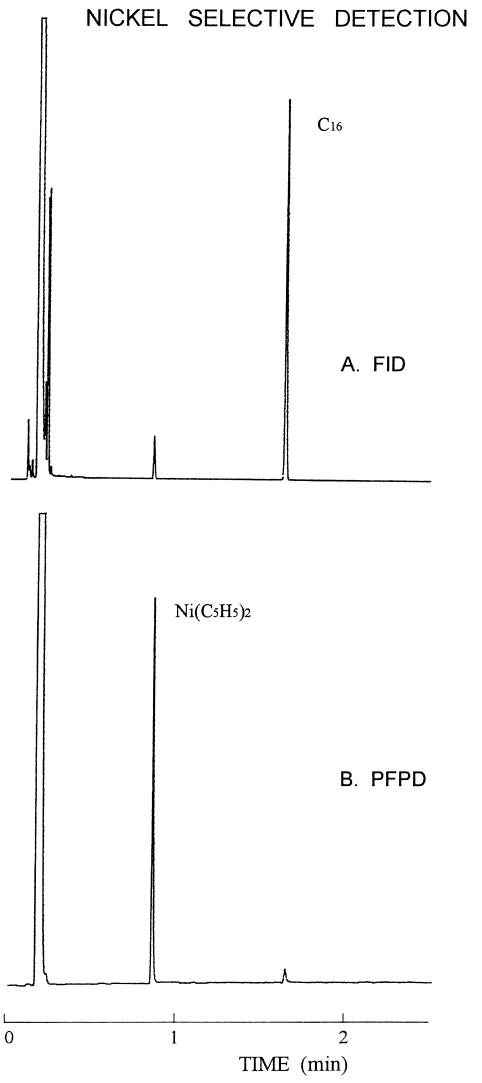

Fig. 44. Nickel selective detection with the PFPD. 0.6 μl of a toluene solution of $1.3 \cdot 10^{-4}$ nickelocene, and 0.1% hexadecane was injected with a split ratio of 80:1. The column was temperature programmed from 80 to 190°C at 50°C/min. An R647 PMT and GG495 filter were used with the PFPD. The PFPD base temperature was 300°C.

it roughly covered the 400–600 nm visible range. Either GG495 filter with R647 PMT or OG590 filter with R1463 PMT could be used for better selectivity.

As shown in Fig. 52, clean GC peak shape was observed for the detection of Bi. A PFPD temperature of 280°C was used. The MDL was around 100 pg Bi/s with the OG590/R1463 PMT and about 70

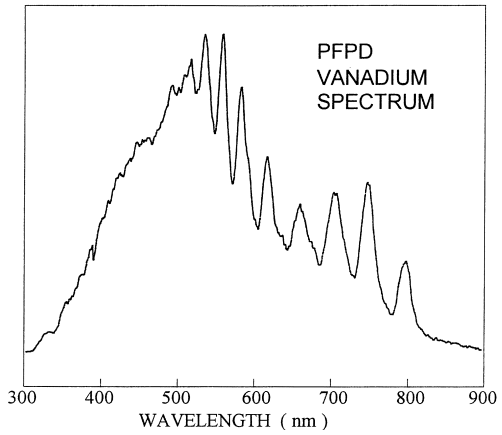

Fig. 45. PFPD undelayed emission spectrum of vanadium. Vanadium(III) acetylacetonate was introduced into the PFPD at 150°C. A WG335 filter was used at the entrance of the monochromator to suppress second-order dispersion.

pg Bi/s with the GG495/R647 PMT combination, which is better than that reported for a conventional FPD [15].

$Bi(C_6H_5)_3$ was used and found to be a stable compound when dissolved in toluene. The PFPD is recommended mostly for inorganic Bi compounds such as BiH_3 or $BiCl_3$ due to its limited selectivity and lower detectivity than a FID.

3.3. PFPD detection of non-metal elements with undelayed emissions

Carbon, boron and silicon are three main-group elements that can be detected with the PFPD through their undelayed emissions.

3.3.1. Universal carbon detection with the PFPD

Hydrocarbons and other organic compounds can be detected with the PFPD with moderate sensitivity. It can thus provide a ''free'' FID-like channel simultaneously with sulfur and other elements that exhibit time-delayed emissions. The significance of having a carbon channel concurrent with an additional element mode of an FPD has been recognized since 1966 [14,44,46,55].

The emission spectrum of carbon is shown in Fig. 53. The spectrum was found to be identical with both aromatic (toluene) and aliphatic (decane) hydrocarbons. The three large bands at 432 nm, 472 nm and

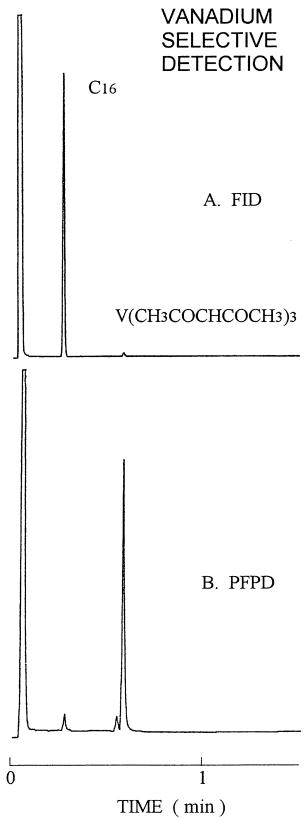

Fig. 46. Vanadium selective detection with the PFPD. 0.5 μl of a 2,4-pentanedione solution of $9 \cdot 10^{-4}$ vanadium(III) acetylacetonate, and 1% hexadecane was injected with a split ratio of 40:1. The column temperature was ramped from 160 to 190°C at 20°C/min. An R1463 PMT and OG590 filter were used with the PFPD. The PFPD base temperature was 320°C.

516 nm are due to the emissions of CH, and C_2 (the two Swan bands), respectively. The latter two seem to favor an air-rich flame and may result in non-linearity, and they could be one of the reasons for the known fact that, in FPD, aromatics produce stronger responses than aliphatic and alicyclic hydrocarbons [3,29]. In fact, none of the Swan bands showed up unambiguously in the FPD [29] where naphthalene showed a considerably higher portion in the green region than dodecane. However, the spectrum shown in Fig. 53 is quite similar to that obtained by Zado and Juvet [4]. Thus, the best filter chosen was BG12. No delayed emission was observed under any conditions.

Hydrogen-rich gas compositions similar to that

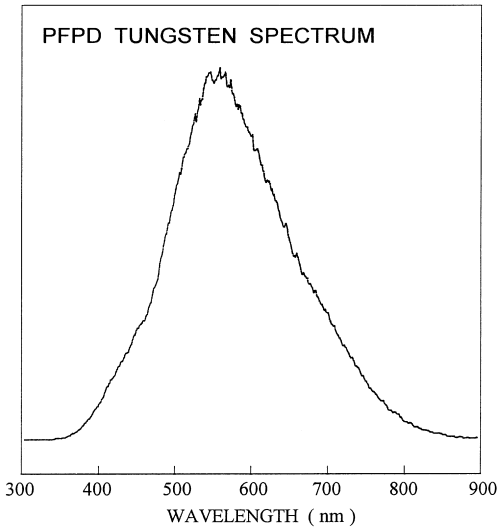

Fig. 47. PFPD undelayed emission spectrum of tungsten. Tungsten was introduced into the detector as tungsten hexacarbonyl at 70°C. The maximum emission wavelength is at about 550 nm.

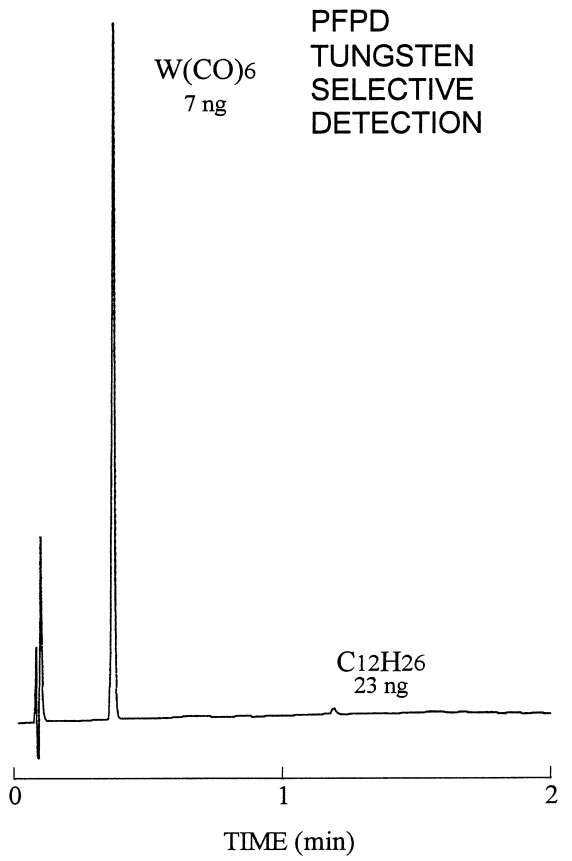

Fig. 48. Tungsten selective detection with the PFPD. 0.7 μl of an ethanol–acetone solution of 0.1% tungsten hexacarbonyl and 0.33% dodecane was injected with a split ratio of 100:1. The column was maintained at 60°C for 0.2 min, and then ramped to 140°C at 40°C/min. An R5070 PMT and GG495 filter were used with the PFPD. The PFPD base temperature was 280°C.

used for sulfur selective detection was optimal for carbon detection. Very air-rich gas compositions are also optional for carbon selective detection and the choice depends on other requirements of selectivity and/or dual element detection.

Clean peak shape is demonstrated for carbon detection in Fig. 54. The MDL was about 100–200 pg C/s and varied with gas composition. Linear response with a limited linear dynamic range of about 2–3 decades was obtained.

Good emission time separation from sulfur was achieved, where the sulfur contribution at the carbon undelayed gate could be less than 0.5%. Phosphorus emission was partially observed in the PFPD carbon channel located at the pulsed flame main emission. Nitrogen emission was about 20-times stronger than that of carbon and can be used for nitrogen identification in comparison to the FID. A relatively low PFPD temperature of 150°C can be used to reduce the flame background. Simultaneous carbon and sulfur PFPD analysis of gasoline was previously reported [44].

3.3.2. Boron

Boron can be selectively detected with the PFPD with medium selectivity.

As illustrated in Fig. 55, boron showed a highly structured spectrum in the green (400–600 nm) range as reported in the literature [26,56]. Since no delayed emission was observed, only undelayed emission was detected. The best sensitivity was achieved with a GG495 filter with an observed MDL of 4 pg B/s. The actual value obtained with the PFPD and our prepared solutions was 6 pg B/s, but boron compound hydrolysis was observed, and recalibration with the FID gave an MDL of 2 pg B/s. Thus, an average of 4 pg B/s was selected. With the WG345 filter, both the signal and the noise increased by about a factor of 2 so that the MDL was about the same while the selectivity was reduced by a factor of 2.5. A 3 mm I.D. combustor was preferred and

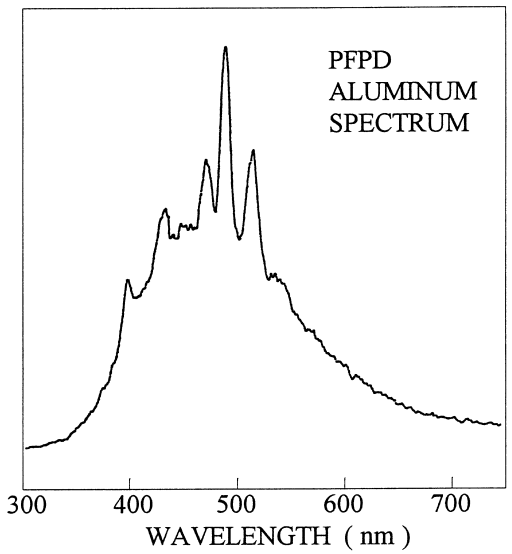

Fig. 49. PFPD undelayed emission spectrum of aluminum. Aluminum was introduced into the detector as aluminum(III) acetylacetonate at 200°C. A WG335 high pass filter was used at the entrance of the monochromator to suppress second-order dispersion.

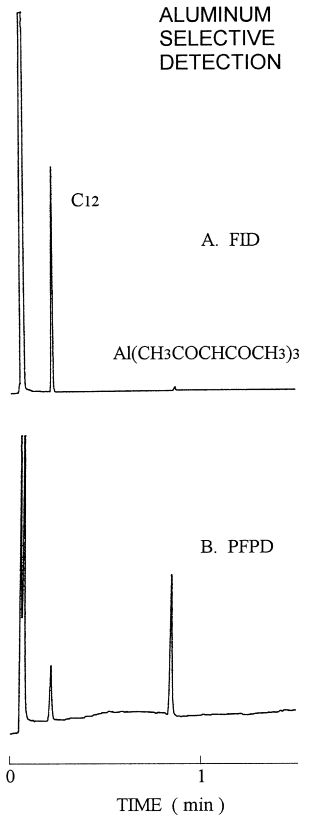

Fig. 50. Aluminum selective detection with the PFPD. 0.5 μl of a 2,4-pentanedione solution of $4 \cdot 10^{-4}$ aluminum(III) acetylacetonate and 1% dodecane was injected with a split ratio of 40:1. The column temperature was kept at 120°C for 0.2 min and then ramped to 190°C at 50°C/min. An R647 PMT and GG495 filter were used with the PFPD. The PFPD base temperature was 320°C.

showed a factor of 2 higher response than a 2 mm I.D. combustor. With a GG495 filter, the B/C selectivity was 640. We did not study the selectivity against S and P but the air-rich gas conditions seem promising. As shown in Fig. 56, a clean peak shape was observed for the PFPD selective detection of boron.

Boron detection is strongly preferential to air-rich gas compositions in marked contrast to normal S, P and N operation. This flame gas composition dependence was similarly reported with conventional FPDs [26,57]. In addition, we note that although our PFPD working temperature was 350°C, lower temperatures (200°C) could be used with similar performance.

3.3.3. Silicon

Silicon can be selectively detected with the PFPD with reasonable sensitivity and limited selectivity against hydrocarbons.

As shown in Fig. 57, silicon exhibited an unstructured broad band emission in the 380–520 nm spectral range. The emission above 610 nm was the result of the second-order dispersion in the monochromator and should be ignored. No delayed emission was observed between 345–800 nm. This severely limits the silicon detection selectivity, but is fortunate as it also prevents column bleeding effects in S, P and other heteroatom selective detection. The best filter overall was the GG495, however, a WG345 or BG12 filter could also be used with higher signal (2.5-times with the WG345) but correspondingly higher noise. Thus, the GG495 is preferred due to its higher selectivity.

We observed, with the GG495 filter, a Si/C selectivity of 120. With the WG345, it was reduced by a factor of 2.2, and with the BG12 by a factor of 3.3. With the OG570 the selectivity was further increased by a factor of almost 2, and with the R5070 PMT and RG695 filter the Si/C selectivity

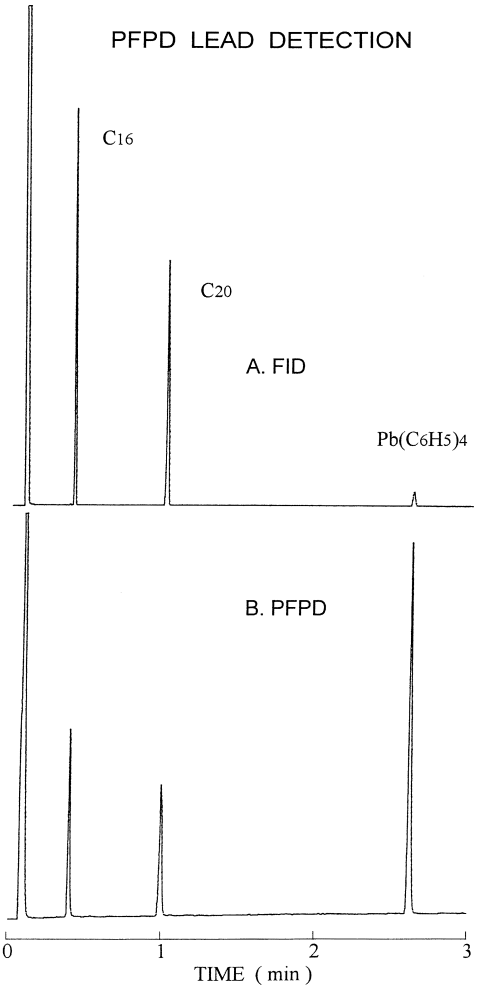

Fig. 51. Lead (selective) detection with the PFPD. 0.5 μl of a solution of $6.7 \cdot 10^{-3}$ hexadecane and eicosane, and $1 \cdot 10^{-3}$ tetraphenyllead was injected with a split ratio of 50:1. The column temperature was ramped from 150 to 270°C at 40°C/min. An R647 PMT, BG12 filter, 350°C detector base temperature and 3 mm I.D. combustor were used with the PFPD.

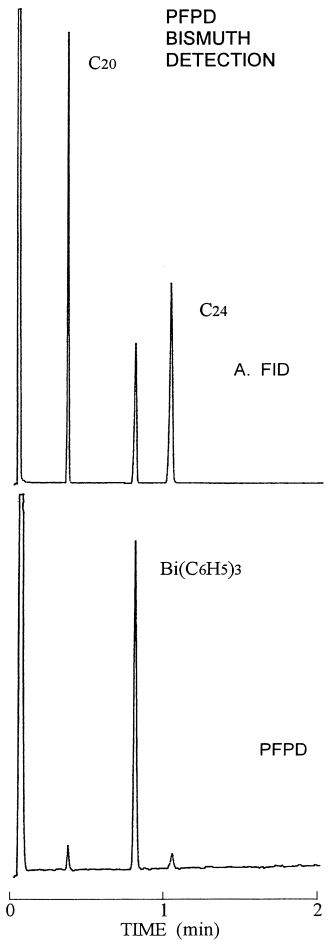

Fig. 52. Bismuth (selective) detection with the PFPD. 0.5 μl of a toluene solution of 0.3% triphenylbismuth, eicosane and tetracosane was injected with a split ratio of 30:1. A 3 m column was used and temperature programmed from 180 to 220°C at 20°C/min. An R1463 PMT and OG590 were used with the PFPD. The PFPD base temperature was 280°C.

became 500 but the MDL was increased by a factor of about 2.

The MDL was found to be about 3 pg Si/s and strongly depends on the pulsed flame stability. Silicon prefers air-rich gas conditions similar to boron and in marked contrast to S and P. A 3 mm I.D. combustor is preferred and yields 1.7-times higher response than that with a 2 mm I.D. combustor. As shown in Fig. 58 a clean GC peak shape was obtained. A 300°C PFPD temperature is recommended but the Si response is practically temperature independent.

It seems that silicon compounds enhance normal FID response [58]. If this observation is correct, both the silicon detection sensitivity and selectivity may actually be better by up to a factor of 3.

3.4. Multi-heteroatom identification and simultaneous selective detection

As described previously [45], a dual gate ap-

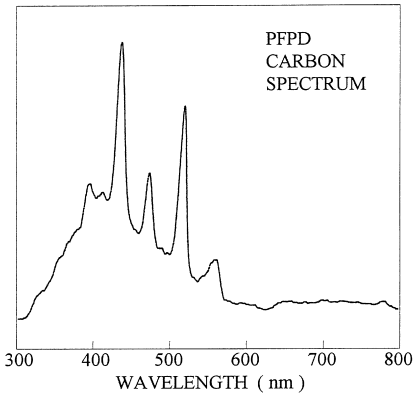

Fig. 53. PFPD undelayed emission spectrum of carbon. Decane was introduced into the PFPD at 70°C. A WG335 high pass filter was used at the entrance of the monochromator to suppress second-order dispersion.

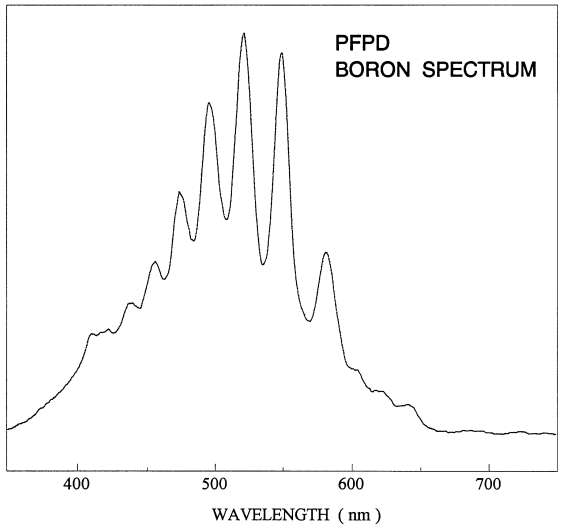

Fig. 55. PFPD undelayed emission spectrum of boron. Tripropylborate was introduced into the PFPD at 100°C. A WG360 high pass filter was used at the entrance of the monochromator to suppress second-order dispersion.

proach, entitled gate response ratio (GRR), can be used for the identification of elements with time-delayed emissions. Briefly, it is based on obtaining two simultaneous chromatograms, each with a different gate delay and/or width. Since the pulsed flame delayed emission time dependence varies from element to element, the ratio of the peak areas in these two chromatograms changes accordingly. This ratio is defined as the GRR. Under certain PFPD conditions, such as its temperature and hydrogen-to-air flow-rate ratio, the GRR value is characteristic of heteroatom elements, and can be used for their identification and detection as demonstrated in Fig. 59. The relative gate positions are roughly shown in the two small inserts. Both gate A and B were placed on the time-delayed emissions, while the latter was further delayed than the former by 4 ms so that the upper trace (obtained by using gate A) in this figure collected mostly the short delayed emissions and the lower trace (obtained by using gate B) contained the longer delayed emissions. The width of gate B was broader than that of gate A to cover the entire long delayed emission region. The GRR is defined here as the ratio of the response of gate B to that of gate A. Therefore, the greater the long delayed emission of an element, the greater its GRR. In addition, a wide-band WG345 filter with a red-sensitive R5070 PMT was used, which provided the spectral measurement conditions for all of these elements.

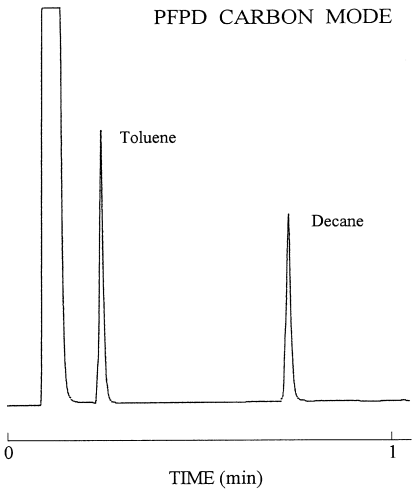

Fig. 54. Universal carbon detection with the PFPD. 0.5 μl of an ethanol solution of $3 \cdot 10^{-3}$ toluene and decane was injected with a split ratio of 50:1. The column temperature was ramped from 50 to 100°C at 40°C/min. An R647 PMT and BG12 filter were used with the PFPD with a short undelayed gate. The PFPD base temperature was 320°C.

Based on the GRR of sulfur, which is normalized to 1, the GRRs obtained for Ge, N, Se, S plus P (as in methyl parathion), P and As are 0.15, 0.10, 0.80, 0.45, 0.25 and 2.0, respectively. The delayed emis-

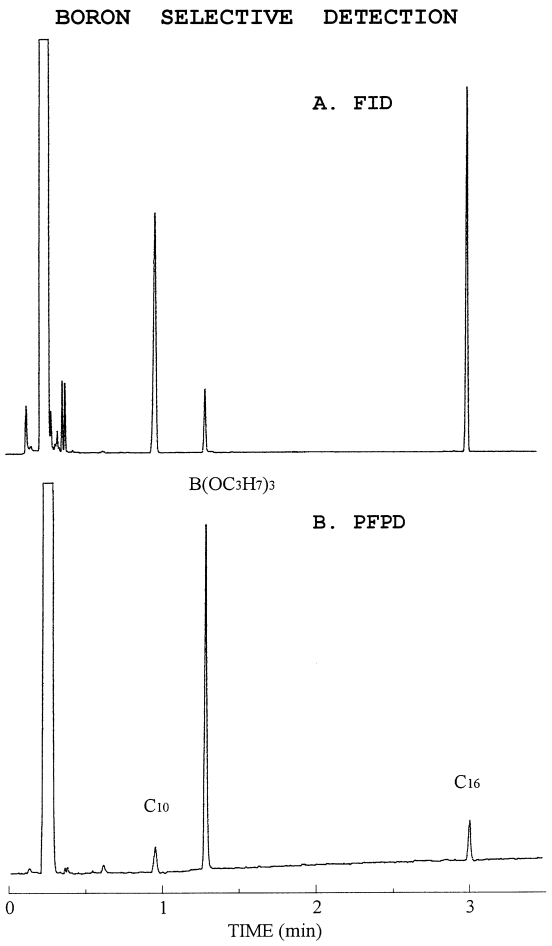

Fig. 56. Boron selective detection with the PFPD. 0.5 μl of a freshly prepared toluene solution of $3 \cdot 10^{-3}$ tripropylborate, decane and hexadecane was injected with a split ratio of 50:1. The column temperature was kept at 60°C for 1 min, then ramped to 190°C at 50°C/min. A very air-rich gas composition and short undelayed gate were used with the PFPD with an R647 PMT and GG495 filter. The PFPD base temperature was 350°C.

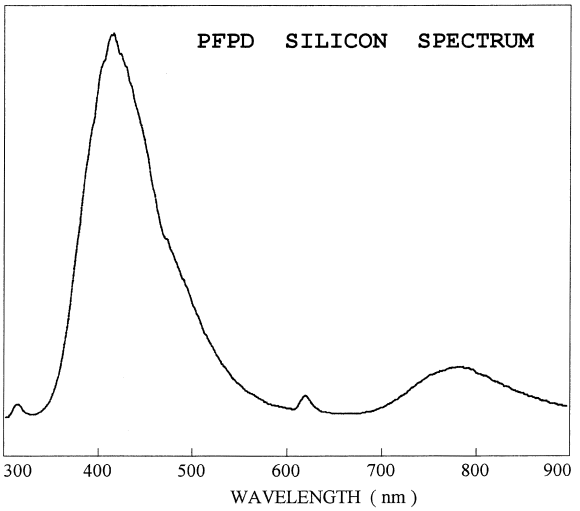

Fig. 57. PFPD undelayed emission spectrum of silicon. Silicon was introduced into the detector as methylphenyldimethoxysilane at 70°C. The second-order dispersion from the monochromator is observed above 600 nm.

sion of As is very long and its maximum is situated toward the longer delayed side as shown in Fig. 5. Therefore, it has the largest GRR which is well over the normalized GRR of S. On the other hand, N has the smallest GRR value of 0.10 because it has the shortest emission delay. The GRR for Ge is 0.15, which is between the values for N (0.10) and for P (0.25) since its emission delay is about 8 ms between that of N and P, as shown in Fig. 15. S plus P has a GRR of 0.45 which is a weighted average of the GRR for S (normalized to 1) and P (0.25). The GRR of Se is 0.80, which is slightly less than that for S. This can be rationalized by the similarity between their similar emission time profile (slightly shorter for Se) and spectral measurement conditions.

Note also that in Fig. 59, since only time-delayed emissions were collected in both gates, no hydrocarbon interference occurred. The two hydrocarbon compounds, dodecane and dimethylphathalate, both with a concentration of $3 \cdot 10^{-3}$, did not appear in either GC trace. The higher selectivity of the PFPD eliminates the hydrocarbon response, combined with multi-heteroatom simultaneous detection.

The GRR can be readily obtained by using the PFPD software [47], or a dual-gated amplifier with a two-channel integrator. It is easy, simple and inexpensive to use. Similarly, an additional manipulation of the pulsed flame emission time dependence is based on using a dual gate subtraction (DGS) method [45]. This DGS method can provide enhanced inter-heteroatom selectivity which in turn results in an element content ratio like S/P in compounds that contain both elements [59]. For hydrocarbons, a simultaneous FID-like channel can be provided by the PFPD [44] that can also be easily obtained by a post-run of the PFPD software [47]. By calculating the PFPD/FID ratio, as performed

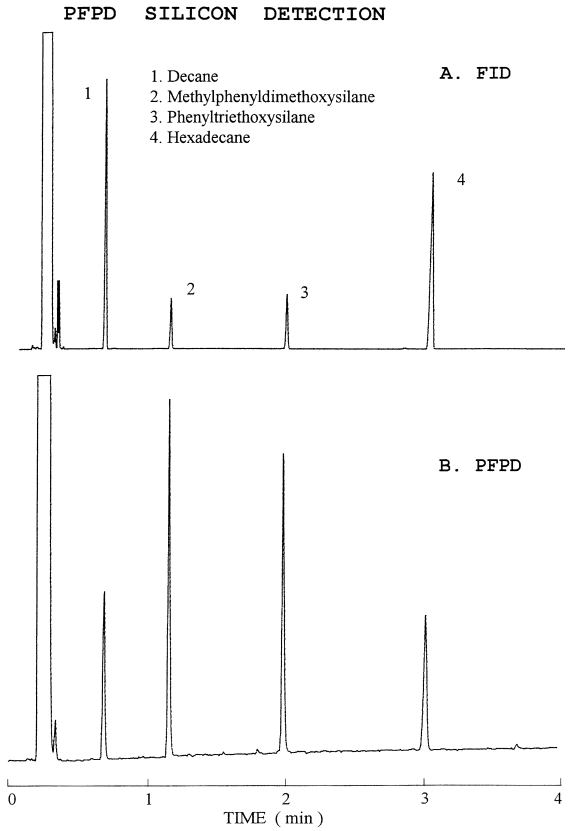

Fig. 58. Silicon selective detection with the PFPD. 0.5 μl of a toluene solution of $3{\cdot}10^{-4}$ methylphenyldimethoxysilane and phenyltriethoxysilane, $3{\cdot}10^{-3}$ decane and hexadecane was injected with a split ratio of 20:1. The column was kept at 70°C for 0.5 min and then ramped to 180°C at 30°C/min. A very air-rich gas composition was used with the PFPD with an R647 PMT and GG495 filter. The PFPD base temperature was 300°C.

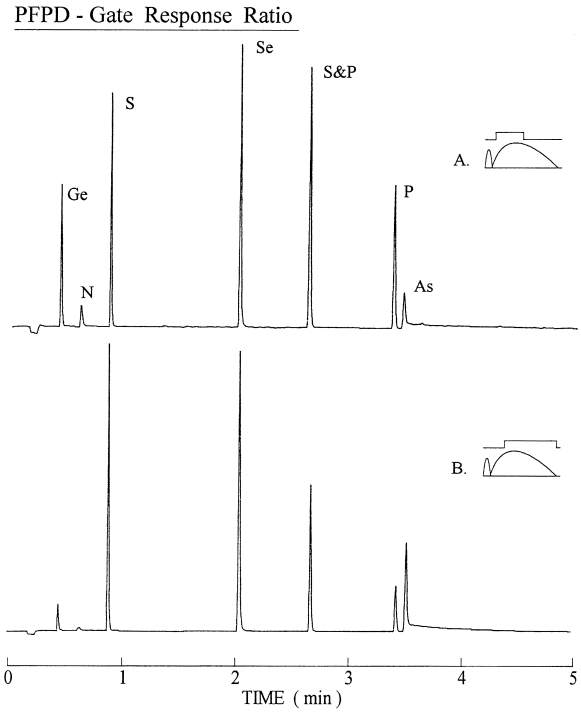

Fig. 59. PFPD multi-heteroatom identification and selective detection. 0.5 μl of a toluene solution of $3{\cdot}10^{-5}$ tetraethylgermanium, $1{\cdot}10^{-3}$ nitrobenzene, $1{\cdot}10^{-5}$ benzothiophene, $3{\cdot}10^{-3}$ dodecane, $3{\cdot}10^{-3}$ dimethyl phthalate, $9{\cdot}10^{-5}$ diphenylselenide, $2{\cdot}10^{-5}$ methyl parathion, $1.3{\cdot}10^{-5}$ triphenyl phosphine and $6{\cdot}10^{-4}$ triphenylarsine was injected with a split ratio of 50:1. The column temperature was ramped from 60 to 250°C at 50°C/min. An R5070 PMT with WG345 filter was used. The two chromatograms were obtained simultaneously with different gate positions by using a double gated amplifier. A 5 ms delay and 10 ms wide gate was used in trace A, whereas in trace B, a 9 ms gate delay was used with a gate width of 20 ms.

with an FPD [55], additional information on the heteroatom/carbon content ratio in a compound can be provided for further compound or element identification [60]. The GRR, DGS, and the element content ratio can all be achieved using the PFPD software [47] by a post-run manipulation of the gate positions.

The time-dependent emission in the pulsed flame enables the effective use of this newly added dimension of information for elements with delayed emissions. However, since many elements (15 out of the 28 studied) are characterized by prompt emission only, without time delay, the GRR approach can not be universally employed and the identification of these elements must be based on their characteristic flame emission spectra as in conventional FPDs. Aue and co-workers [25–27,30,61] have developed a spectral response ratio measurement method for element identification, based on the element unique photometric response in a dual PMT FPD having two different filters. Although this spectral response ratio was used with an FPD with two PMTs, it can be used with any FPD including the PFPD while performing two consecutive chromatograms, each with a different filter in front of the PMT. This spectral response ratio method enables element identification for all the 28 elements that are detectable with the PFPD.

4. Conclusions

The PFPD selective detection of 28 elements was systematically investigated, and their detection limits, selectivities against carbon and other practical aspects of experimental details are presented in this paper. The general characteristics of the PFPD selective detection of these elements are as follows:

1. Similar to conventional FPDs, the PFPD detectable elements are widely distributed around the periodic table except for group VIII (i.e., the rare gases), while those in the first two groups, IA and IIA, could probably be detected if their compounds were gas chromatographable.
2. Because of its broad range of heteroatom detectability, the PFPD can be regarded as a semi-universal heteroatom selective detector for GC, with higher sensitivities and selectivities than are achievable with the conventional FPD for elements with delayed emissions.
3. The time-delayed emissions available with the PFPD for 13 elements enable a unique gate response ratio approach for multi-heteroatom simultaneous detection and identification. For those elements with undelayed emissions, the spectral response ratio method can be used as reported with conventional FPD.
4. The ease of use, small bench space required, low gas consumption, and simplicity of operation and maintenance of the PFPD make it an economical alternative to the atomic emission detector, with better sensitivity and selectivity for certain important elements, such as S, P and Sn.
5. Chlorine, as well as fluorine, iodine, hydrogen, oxygen, mercury and zinc remain undetectable with the PFPD. Halogens can be detected via indium sensitization but this approach was found to have long-term instability problems.
6. The volatility, thermal lability, hydrolysis property and even the availability of some heteroatom compounds could be considered as constrains. Therefore, care must sometimes be exercised in practice so that the loss of heteroatom compounds prior to their entering the detector is minimized through the use of a short column and/or a higher carrier gas flow-rate.
7. The dual gate subtraction method for improved inter-heteroatom selectivity can be achieved using the PFPD software.
8. Although the PFPD has been used in many applications, such as sulfur detection in petrochemical fluids and pesticide analysis, further application of the PFPD for the selective detection of elements besides S and P is advocated by this paper.

Acknowledgements

This research was supported by a grant from the Israel Science Foundation. Dr. Albert Danon's contribution to this work in its early stages is greatly appreciated. We are grateful to Dr. Samuel B. Wainhaus for his painstaking proofreading of the manuscript.

References

[1] R.S. Juvet, R.P. Durbin, J. Gas Chromatogr. 1 (1963) 14.
[2] R.W. Moshier and R.E. Sievers, Gas Chromatography of Metal Chelates, Pergamon Press, Oxford, 1965.
[3] R.S. Juvet, R.P. Durbin, Anal. Chem. 38 (1966) 565.
[4] F.M. Zado, R.S. Juvet, Anal. Chem. 38 (1966) 569.
[5] G. Guiochon and C. Pommier, Gas Chromatography in Organics and Organometallics, Ann Arbor Science Publishers, Ann Arbor, MI, 1973.
[6] P.C. Uden, J. Chromatogr. 313 (1984) 3.
[7] K. Robards, E. Patsalides, S. Dilli, J. Chromatogr. 411 (1987) 1.
[8] T.M. Dowling, P.C. Uden, J. Chromatogr. 644 (1993) 153.
[9] W.A. Aue, C.G. Flinn, J. Chromatogr. 142 (1977) 145.
[10] D.L. Klayman and W.H.H. Günther, Organic Selenium Compounds: Their Chemistry and Biology, Wiley, New York, 1973.
[11] N.O. Korolkoff, Solid State Technol. 32 (1989) 49.
[12] J.H. Harwood, Industrial Applications of the Organometallic Compounds, Chapman and Hall, London, 1963.
[13] M. Dressler, Selective Gas Chromatographic Detectors, Elsevier, Amsterdam, 1986.
[14] S.S. Brody, J.E. Chaney, J. Gas Chromatogr. 4 (1966) 42.
[15] W.A. Aue, C.R. Hastings, J. Chromatogr. 87 (1973) 232.
[16] C.G. Flinn, W.A. Aue, J. Chromatogr. 153 (1978) 49.
[17] W.A. Aue, C.G. Flinn, J. Chromatogr. 158 (1978) 161.
[18] C.G. Flinn, W.A. Aue, J. Chromatogr. 186 (1979) 299.
[19] C.G. Flinn, W.A. Aue, J. Chromatogr. Sci. 18 (1980) 136.
[20] W.A. Aue, C.G. Flinn, Anal. Chem. 52 (1980) 1537.
[21] X.-Y. Sun, W.A. Aue, J. Chromatogr. 467 (1989) 75.
[22] X.-Y. Sun, W.A. Aue, Can. J. Chem. 67 (1989) 897.
[23] X.-Y. Sun, W.A. Aue, Mikrochim. Acta (Wien) I (1990) 1.
[24] W.A. Aue, X.-Y. Sun, J. Chromatogr. 633 (1993) 151.
[25] W.A. Aue, B. Millier, X.-Y. Sun, Anal. Chem. 63 (1991) 2951.

[26] W.A. Aue, X.-Y. Sun, B. Millier, J. Chromatogr. 606 (1992) 73.
[27] B. Millier, X.-Y. Sun, W.A. Aue, Anal. Chem. 65 (1993) 104.
[28] W.A. Aue, B. Millier, X.-Y. Sun, Anal. Chem. 62 (1990) 2453.
[29] X.-Y. Sun, B. Millier, W.A. Aue, Can. J. Chem. 70 (1992) 1129.
[30] W.A. Aue, B. Millier, X.-Y. Sun, Can. J. Chem. 70 (1992) 1143.
[31] C.V. Overfield, J.D. Winfordner, J. Chromatogr. Sci. 8 (1970) 233.
[32] M.C. Bowman, M. Beroza, J. Chromatogr. Sci. 9 (1971) 44.
[33] G. Wells, Anal. Chem. 55 (1983) 2112.
[34] M.C. Bowman, M. Beroza, J. Chromatogr. Sci. 7 (1969) 484.
[35] Y.-Z. Tang, W.A. Aue, J. Chromatogr. 408 (1987) 69.
[36] A.V. Nowak, H.V. Malmstadt, Anal. Chem. 40 (1968) 1108.
[37] P.C. Uden (Editor), Element-Specific Chromatographic Detection by Atomic Emission Spectroscopy (ACS Symposium Series No. 479) ACS, Washington, DC, 1992.
[38] Hewlett-Packard Atomic Emission Detector, Listing of Publications, February 1995.
[39] B.D. Quimby, J.J. Sullivan, Anal. Chem. 62 (1990) 1027.
[40] S.E. Eckert-Tilotta, S.B. Hawthorne, D.J. Miller, J. Chromatogr. 591 (1992) 313.
[41] J.J. Sullivan, B.D. Quimby, Anal. Chem. 62 (1990) 1034.
[42] A. Amirav, Israel Pat. 95 617; US Pat. 5 153 673; Eur. Pat. 0 475 250 and Japan Pat. Application.
[43] E. Atar, S. Cheskis, A. Amirav, Anal. Chem. 63 (1991) 2061.
[44] S. Cheskis, E. Atar, A. Amirav, Anal. Chem. 65 (1993) 539.
[45] A. Amirav, H. Jing, Anal. Chem. 67 (1995) 3305.
[46] N. Tzanani, A. Amirav, Anal. Chem. 67 (1995) 167.
[47] A. Amirav and B. Leibovici, The PFPD Software (1995). A demonstration disk of the PFPD software is available upon request.
[48] P.L. Patterson, in H.H. Hill and D.G. McMinn (Editors), Detectors for Capillary Chromatography, Wiley, New York, 1992, p. 158.
[49] S. Kapila, C.R. Vogt, J. Chromatogr. Sci. 17 (1979) 327.
[50] P.T. Gilbert, in R. Mavrodineanu (Editor), Analytical Flame Spectroscopy, Macmillan, London, 1970, p. 299.
[51] J.A. Jacobsen, F. Stuer-Lauridsen, G. Pritzl, Appl. Organomet. Chem. 11 (1997) 737.
[52] H.H. Hill, W.A. Aue, J. Chromatogr. 74 (1972) 311.
[53] W.A. Aue, H.H. Hill, Anal. Chem. 45 (1973) 729.
[54] R. Ross, T. Shafik, J. Chromatogr. Sci. 11 (1973) 46.
[55] H.W. Grice, M.L. Yates, D.J. David, J. Chromatogr. Sci. 8 (1970) 90.
[56] P.T. Gilbert, in R. Mavrodineanu (Editor), Analytical Flame Spectroscopy, Macmillan, London, 1970, p. 190.
[57] E.J. Sowinski, I.H. Suffet, J. Chromatogr. Sci. 9 (1971) 632.
[58] J.T. Scanlon, D.E. Willis, J. Chromatogr. Sci. 23 (1985) 333.
[59] H. Jing, A. Amirav, Anal. Chem. 69 (1997) 1426.
[60] A. Amirav and H. Jing, Pulsed Flame Photometer Detector for Gas Chromatography, (booklet, available upon request), Tel Aviv University, 1997.
[61] H. Singh, B. Millier, W.A. Aue, J. Chromatogr. A 687 (1994) 291.